ANTIOXIDANT ELECTROSPUN FIBER MATS OF HYDROGEN-BONDED POLYMER COMPLEXES

A Thesis

by

ADWAIT SANJAY GAIKWAD

Submitted to the Office of Graduate and Professional Studies of
Texas A&M University
in partial fulfillment of the requirements for the degree of

MASTER OF SCIENCE

Chair of Committee,	Svetlana Sukhishvili
Committee Members,	Terry Creasy
	Jodie Lutkenhaus
Head of Department,	Ibrahim Karaman

August 2019

Major Subject: Materials Science and Engineering

ABSTRACT

We report on highly functional, electrospun fibers of hydrogen-bonding polymers which exhibit composition-dependent mechanical properties and sustained antioxidant activity. The fibers were electrospun from dimethylformamide (DMF)/dimethyl sulfoxide (DMSO) mixed solutions containing polyvinylpyrrolidone (PVP) (Mw 1300, 360 and 55 kDa) and a hydrogen-bonding antioxidant partner, tannic acid (TA). The fiber diameters were controlled by PVP concentration and ranged between 380 ± 50 to 750 ± 70 nm for fibers with equimolar ratio of PVP-TA hydrogen-bonding units prepared using 10.5 to 15 weight % PVP. Hydrogen bonding between PVP and TA was revealed by differential scanning calorimetry (DSC) as suppression of the glass transition temperature (Tg) of PVP-TA assemblies within temperature up to 225 ^{o}C, as compared that of pristine PVP fibers with Tg of 178 ^{o}C. Due to the presence of network of hydrogen bonds, PVP-TA fibers exhibited enhanced tensile strength and Young's moduli, as well as decreased elongation at break as compared with fibers made of pristine PVP. The mechanical properties of PVP-TA fibers were strongly dependent on the component ratio. A maximum in the tensile strength occurred for the 0.25 molar fraction of TA hydrogen-bonding units to those of PVP, where number of hydrogen bonds in the system was maximized. At the same time, the elongation at break monotonously decreased as fibers became more enriched with TA. The component ratio also strongly affected the stability of the fibers in aqueous solutions. In acidic medium, the PVP/TA fibers were stable over the widest range of compositions. At neutral pH values, the fiber stability had stronger dependency on composition. While excess amounts of PVP resulted in fiber swelling and disintegration after exposure to water, the presence of equimolar amount or two-fold molar unit excess of TA provided stabilization/integrity to the fibers for at least 50 days. Importantly,

PVP-TA fiber mats exhibited strong, prolonged antioxidant activity supported by the assembled polyphenol (TA), showing promise for their application for scavenging free radicals in solution.

DEDICATION

To God, I can do all things through him which gives me strength.

To my parents, Dr. Sanjay Gaikwad and Mrs. Neha Gaikwad, who showed me how to love, taught me the importance and education, always encourages me to pursue my dreams and supported me in immeasurable ways throughout it all.

To my grandfathers, Dr. Vinayakrao Gaikwad and Mr. Nandlal Dharam, you were lifelong teachers. To my grandmothers, Mrs. Sunanda Gaikwad and Mrs. Vijaya Dharam, your life experiences are what led me to become a materials engineering.

To my friends, I never would have made it this far without all of your love and support. Thanks for making me laugh so hard I cry and for helping me to enjoy life always!

ACKNOWLEDGEMENTS

This thesis was a true test of my abilities as a student and researcher, and one of the most difficult tasks I have undertaken. I would not have been able to complete this thesis without the support and guidance I received from the people around me who I would like to sincerely thank and acknowledge.

First and foremost, I would like to thank my advisor, Dr. Svetlana Sukhishvili, without her advice, guidance, and instruction, I would never have been able to complete my thesis or succeed in graduate school. She has been so incredibly helpful and very generous with her time and knowledge, anything I ever needed she went above and beyond to help me and gave me opportunities that I will be eternally grateful for. She has successfully guided me from the naive graduate research assistant I once was, to the knowledgeable qualified Master's student I have become. She provided me with many opportunities, making it possible for me to be a teaching assistant and even supported my travel to present our work at the 2018 ACS conference. Her knowledge of the field is immense and she was always able to inspire my continued interest and love of science and chemistry. I sincerely appreciate the support and patience she provided me whenever I had questions, was facing difficulties, or was just plainly taking too long and needed some motivation. She is truly a kind, intelligent, and caring human being and I was extremely fortunate to have the opportunity to have her as my advisor.

Additionally, I would like to thank Dr. Terry Creasy, Dr. Miladin Radovic and Dr. Ibrahim Karaman for providing me with an opportunity for teaching assistantship. They were always willing to help with any questions or problems I had and their knowledge is truly appreciated. I would also like to thank some of the student members of my research group, Parvin Karimineghlani, Hanna Hlushko, Qing Zhou, Victoria Albright, Diana Al-Husseini, Raman

Hlushko, Aliaksei Aliakseyeu and Dr. Viktar Selin who were always available to bounce ideas around with, provide insight, and assist with certain concepts I was unclear on. I would also like to thank my committee member Dr. Terry Creasy and Dr. Jodie Lutkenhaus for being on my committee and supporting me throughout my Masters tenure. In addition, I would also like to thank Dr. Mohammad Naraghi for providing his immense knowledge and wisdom in fiber mechanics; his multifunctional materials class was probably one of the most knowledgeable things I have ever learned about.

Finally, I would like to thank my loving family without them none of this would be possible, they have supported, guided, and inspired me my entire life. My parents have always been truly selfless and provided me with everything I ever needed to succeed and I will forever appreciate their love and support. I would also like to thank my amazing friends for always being there for me and supporting me. Their encouragement and continuous love have helped me through this process and kept me motivated to never give up and always work hard.

Lastly, I would like to thank the Texas A&M University and the Materials Science and Engineering department for creating an institution with an atmosphere that is conducive for research.

CONTRIBUTORS AND FUNDING SOURCES

Contributors

This work was supervised by a thesis committee consisting of Dr. Svetlana Sukhishvili (Advisor), Dr. Terry Creasy (Committee member), of the Department of Materials Science and Engineering and Dr. Jodie Lutkenhaus (Committee member) of the Department of Chemical Engineering.

The data collection and analysis for Chapter 5 was done in Dr. Mohammad Naraghi's lab of the Department of Aerospace Engineering.

Antioxidant properties and pH stability tests in Chapter 4 were conducted by Hanna Hlushko.

All other work conducted for the thesis was completed by the student independently.

Funding Sources

We acknowledge Texas A&M University Experiment Station for the funding. This work was also partially supported by the National Science Foundation under Award DMR-1610725 (S.S.). We acknowledge Materials Characterization Facility for optical and scanning electron microscopy.

NOMENCLATURE

PVP	Poly(vinylpyrrolidone)
TA	Tannic acid
SEM	Scanning Electron Microscopy
IPC	Inter-polymer Complex
TGA	Thermogravimetric analysis
DSC	Differential scanning calorimetry
AFM	Atomic force microscopy
ITC	Isothermal titration calorimetry
DMF	Dimethylformamide
DMSO	Dimethyl sulfoxide
LbL	Layer-by-layer
ABTS	Azino-bis (3-ethylbenzthiazoline-6-sulfonic acid)

TABLE OF CONTENTS

Page

LIST OF FIGURES

Page

CHAPTER I

INTRODUCTION

Introduction to Hydrogen-Bonded Systems

During last several years, many studies have showed the formation and properties of interpolymer polymer complexes (IPC) which is stabilized through either electrostatic interaction (polyanion-polycations) or hydrogen bonding (polyacid-polybase). Baily *et al*. showed that the complexation between polyacids and polyethylene oxide (PEO) are governed by hydrogen bonding and IPC stoichiometry approaches 1:1. These interactions are affected by temperature and pH of the media in which they are being mixed and the molecular weights of the interacting polymers. At low pH (pH<4), phase separation occurs due to strong protonation of hydrogen-donating species and at higher pH they exist as a homogenous solution.

Hydrogen bonds are a special type of dipole-dipole interaction that are neither truly covalent nor ionic, but contain characteristics of both types of bonds. The interaction involves a proton donor and acceptor, X—H•••Y, where X or Y = F, O, or N. The hydrogen is covalently bonded to an electronegative donor "X" and interacts with an electronegative acceptor "Y", which typically contains a lone pair. Hydrogen bonds have been shown to contain energetic contributions from electrostatic polarization, dispersion and exchange repulsion, and a covalent-like charge transfer.[1-3] The enthalpy of a single hydrogen bond is comparatively low (2-15 kJ/mol) and the length of hydrogen bond can fall in the range of 1.2-3.0 A^{o}. However, when there is a simultaneous formation of a large number of intermolecular hydrogen bonds between two macromolecules (cooperative phenomenon) the strength of the interaction is very significant. These strong interactions lead to the ladder type structure and begin packing immediately in order to reduce surface energy associated with solvent molecule and forms a compact hydrogen bonded complex aggregate.

Factors Affecting Hydrogen Bonding

Since hydrogen bonding occurs between proton-accepting groups of non-ionic polymers and non-ionized carboxylic groups of poly(carboxylic acids), the formation of IPC depends on the degree of ionization, *i.e.* pKa of poly(carboxylic acids) and pH of a media.[4] Each complexation system has its own critical pH value at which the complex can be obtained almost stoichiometrically. This critical pH values coincides with the dissociation constants of poly (carboxylic acid). Higher the pKa value, the lower will be the probability of dissociation of carboxylic groups. Therefore, it is considered that larger pKa value results in critical value of the pH value.[4]

Another factor which affects the complexation of IPC is the molecular weight of interacting polymers. Khutoryanskiy *et al.* observed a sharp increase in critical value of pH as molecular weight increases when number of hydrogen are formed.[5]

The nature of solvent also plays an essential role in IPC formation.[6] The thermodynamic parameters of mixing of two interacting polymers can be determined my isothermal calorimetric titration (ITC) measurements. The enthalpy of mixing of two polymers forming IPC depends on a type of solvent. For example, the enthalpy of mixing of PMAA with PVP were found to be positive in water but, negative in N,N-dimethylformamide.[7] The larger the positive value of the mixing of enthalpy, stronger will be the hydrophobic interactions between two polymers driven by positive value of entropy and hence the positive of Gibbs's free energy .

One of the most important factors that influence the interpolymer complexation in solutions is environmental temperature. Hydrogen bonds begin to dissociate at higher temperatures, whereas the contribution of hydrophobic effects into IPC stabilization is getting stronger. Hence, the stability of IPC greatly depends on a delicate balance between the contribution of hydrogen

bonding, hydrophobic effects as well as temperature. The IPC which are formed by the polymers with lower critical solution temperature, are quite stable and form larger aggregates upon heating.[8-10] On the other hand, when the contribution of hydrophobic effects into stabilization of IPC is less important, the complexes dissociate at elevated temperatures.[8-10]

A number of technical applications of hydrogen-bonded IPC have been suggested. These include ion-conducting materials,[11] reagents for prevention of soil erosion,[12] and capture of radioactive elements in soil,[13] emulsifiers, and polymeric membranes.[14-17] Since most of IPC are formed by water-soluble polymers, which are widely used as pharmaceutical excipients, there is a huge potential in application of polymeric complexes in dosage forms design.

CHAPTER II

LITERATURE REVIEW

Introduction to Electrospinning

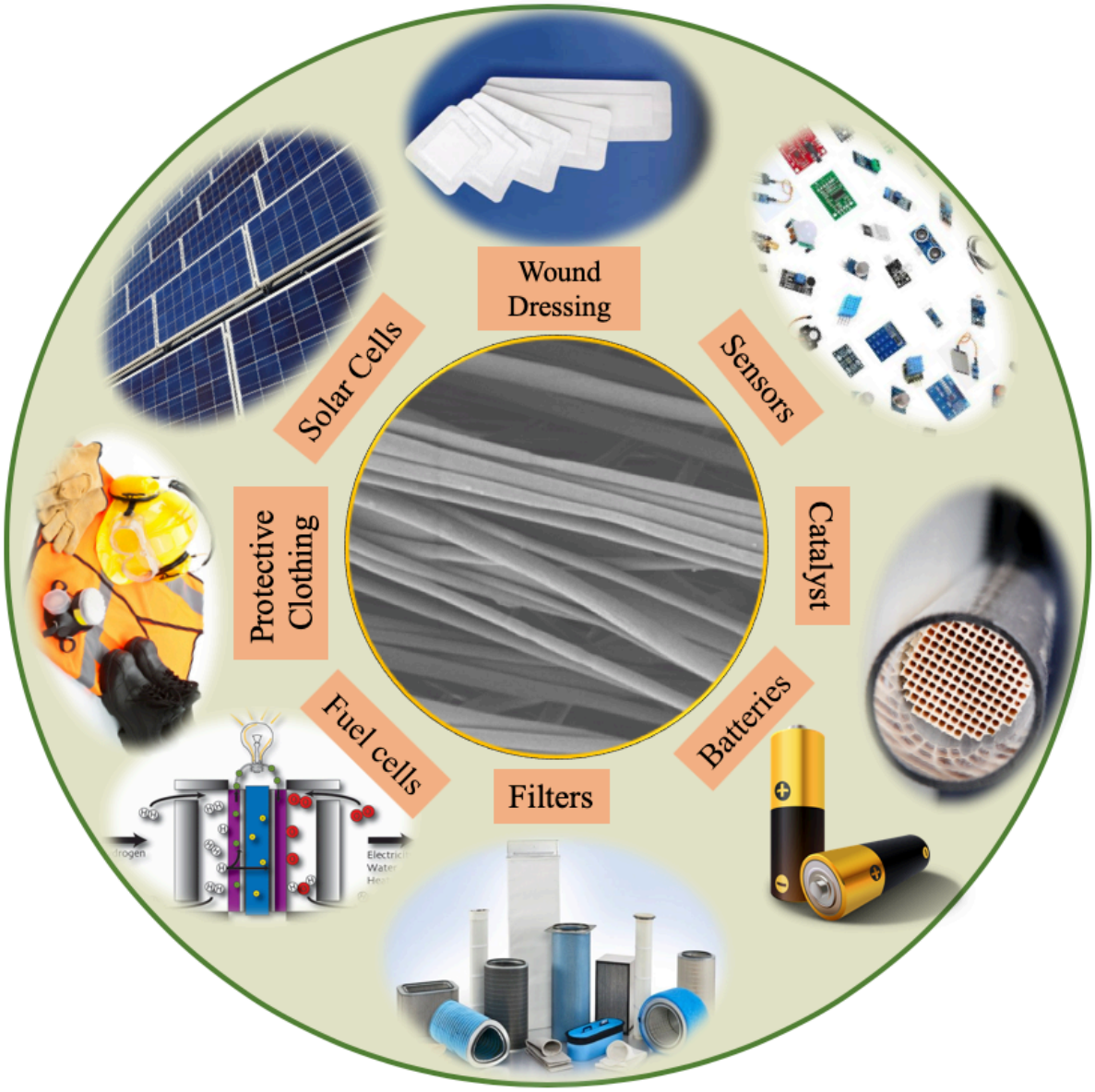

Figure II-1. Applications of nanofibers. Figure was adapted from reference [18].

Electrospinning Overview

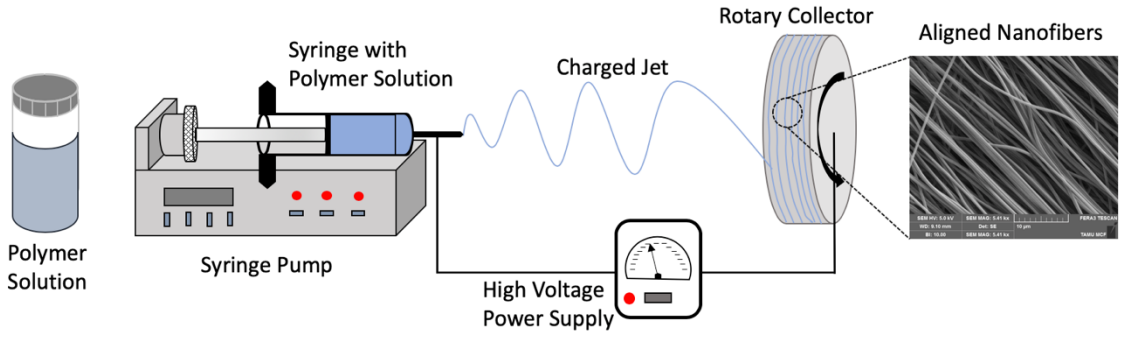

Figure II-2. Schematic representation of electrospinning setup for producing nanofibers from a polymer solution.

Nanosized materials are increasingly becoming popular during recent years in many fields as shown in Figure II-1[18] because of their high surface to volume ratio. Fields such as tissue engineering are taking advantages of their nanosized dimensions which are similar to many biological entities such as viruses, bacteria and proteins.

There are various ways to make such nanofibers mats that include drawing, template synthesis, phase separation, self-assembly, and electrospinning. Electrospinning is of particular interest because of its convenient processing and known reproducibility. It can be used with a wide range of polymers to develop a scaffold that is made up of a porous nanofiber network.

Electrospinning process has three basic components. A schematic of the electrospinning process is shown in Figure II-2.

1. High voltage supplier: This unit supplies direct current (DC), generally. However, it is also possible to use alternating current (AC) potential. Generally the voltage used is between 1 to 30 KV.[16]

2. Spinneret: Typical electrospinning spinneret consists of a single capillary needle in order to obtain nanofibers. These capillary needles can also be configured as single, co-axial and multi-axial phase emitters to obtained nanofibers of respective geometries. The needle is connected to one of the electrodes.
3. Metal collector: Once solidified during the spinning process, electrospun fibers can be collected into a wide variety of collectors, mainly consisting of stationary and rotating platforms. These collectors will have a significant impact in the final design of the electrospun sample. Stationary collectors are commonly flat plates to collect random fibers where the extent of the area can be tailored to a desired range. Rotating collectors include disks, mandrels and drums, all which can have a wide variety of desired diameters. Mandrels can collect fibers in random orientation due to its typically short diameter. Meanwhile, disks and drums are able to collect aligned structures if diameter/length ratio and rotating speed are high enough to allow high linear speeds that will allow stretching of the fibers during collection. The difference in the collectors is shown in Figure II-3.

The process of electrospinning utilizes an external electric field to apply a charge to a small drop of polymer solution that directly opposes the surface tension of the solution. Once the charges overcome the surface tension of the solution, a thin jet of electrically charged solution is created. The jet moves toward the grounded return plate as the solvent evaporates leaving a solid polymer nanofiber that is collected.[19-21] An oval shaped jet is formed is known as a Taylor Cone, which occurs when the critical voltage applied to droplet of solution overcomes the surface tension of the solution, resulting in a thin jet that moves in a conical direction towards the return

electrode.[22, 23] The electrified jet undergoes an elongation continues process, leading the formation of a very long and thin jet that travel towards the collector which is the region of lower potential.

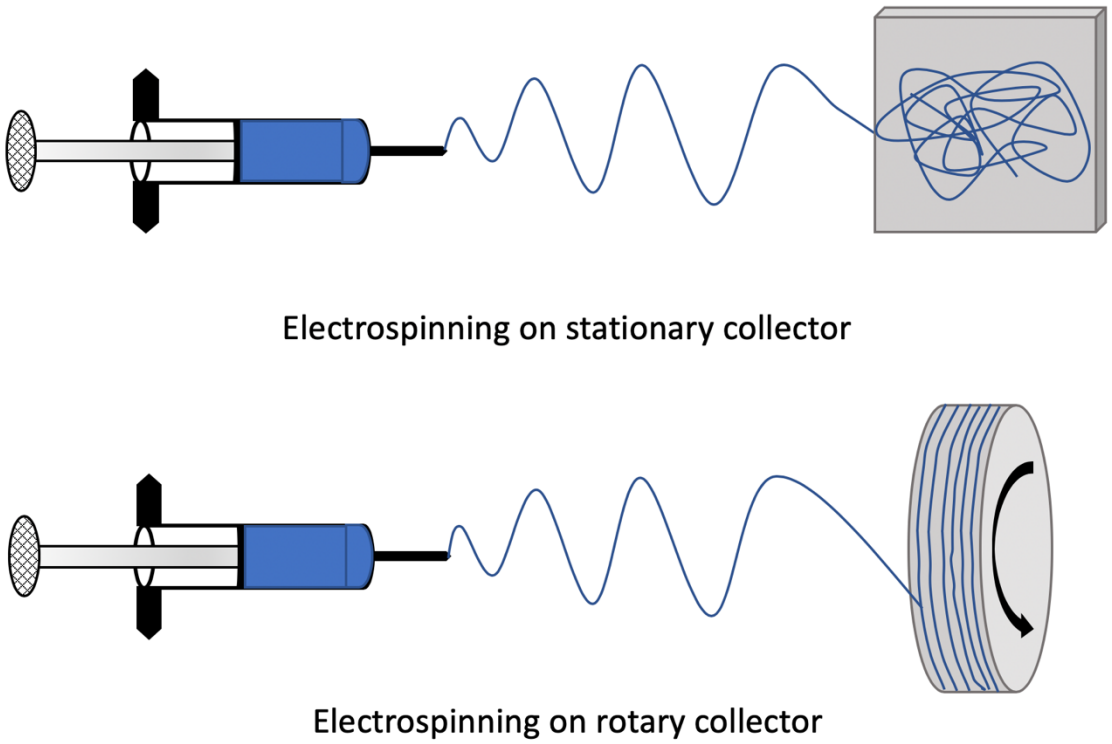

Figure II-3. Schematic representation of two ways to collect electrospun fibers a) flat plate collector b) rotary collector.

As the jet travels towards the collector, due to the stretching, it becomes thinner and thinner. Therefore, as surface area increases, the solvent evaporation rate increases during the trajectory. When nanofiber properties such as morphology, diameter etc. can largely be influenced by various parameters, optimization of the following parameters is necessary to bring down the fiber diameter to nanoscale.[19, 24, 25]:

- Solution parameters: Viscosity, dielectric constant, conductivity, molecular weight of a polymer, concentration of a polymer in a solution, surface tension of a solution.

- Processing parameters: Voltage, solution feed rate in the spinneret, orifice diameter, nature of collector, distance between collector and the tip of the syringe.
- Ambient parameters: Relative humidity, temperature.

Low solution concentration results into the formation of polymeric microparticles. This condition is often be called as collection electrospraying [below 3-5 wt.%]. Increasing the concentration above certain limit will yield fibers with beads in it called nanobeads. At intermediate regime, the formation of continuous robust fibers will occur. Similarly, at high concentration (around 30 wt.%), it becomes difficult to yield fibers with dimensions in nanoscale. An increase in concentration, increases the viscosity of solution. The viscosity generates an opposing force to the electrostatic repulsion during stretching of a fiber. Molecular weight of a polymer largely influences the viscosity of a solution. High molecular weight yields high viscosity of a solution. Therefore, at high viscosity the opposing force will be greater compared to low viscosity solution and hence the fiber diameters will be in large scales.[26]

Solution conductivity plays essential role in spinning the fibers. High dielectric constant of a solvent leads to an increase in conductivity of a solution which will further enhance stretching of the jet due to the presence of more charge carriers.[27] There are many ways to improve the conductivity of a spinning solution. Common practice is either to use solvent with high dielectric constant or incorporate salts into the solution. Using mixtures of a solvent and salt may also help reduce the surface tension of the solution. Low surface tension improves the fiber stretching during electrospinning process.[28]

Stretching force applied on the droplet is due to the applied electric field. Therefore, use of a high voltage increases the stretching force on the droplet and hence the reduction in diameter

occurs. However, when the value of a voltage applied is beyond the required limit, the diameter may actually start to increase due to the reduction in flight time of a fiber.[29-32]

Flight time of a jet also depends on the distance between collector and the tip of the spinneret. Varying this distance affects the electric field strength between the collector and the spinneret. Increasing the distance may decrease the fiber diameter.[33] However, beyond the required distance, fiber diameter may actually start to increase due to the weakening of electric field at a larger distance.[34, 35]

Effect of solution feed-rate on fiber diameter is observed in several studies can either increase or decrease fiber diameter.[36-40] Some studies showed that with increase in feed-rate result in an increase in fiber diameter.[36-38] This is due to increased volume and initial radius of the electrospinning jet leading to reduced bending instability and subsequently increases in fiber diameter. In a study by Schoenmaker *et al.*, the fiber diameter first increased then decreased when the feed-rate was increased.[40] The reduction in average fiber diameter with high feed-rate has been attributed to the occurrence of secondary jets from the main jet as solidified solution at the tip of the nozzle forces jet eruption from unsolidified surfaces. The secondary jets will result in small diameter fibers compared to the initial primary jet.

Raising the temperature of the solution during electrospinning has been shown to reduce fiber diameter.[38] At high solution temperature, the viscosity of the solution will be lowered and this reduces the resistance to stretching under the same stretching force as of at ambient temperature. However, high temperature would also increase the solidification rate of the spinning jet and this may accelerate the "stiffening" of the jet and therefore its resistance to stretching.

Characterization of Nanofibers

Microscopic Studies

Nanofibers are impossible to be seen and characterized with naked eye because of their submicron size. Therefore, microscopic techniques can be used to characterize the properties of nanofibers such as fiber diameter, diameter distribution, orientation and morphology. Surface characterization and porosity may other important parameters to be considered if the application of those fibers fall into such area.[41, 42]

Optical Microscopy

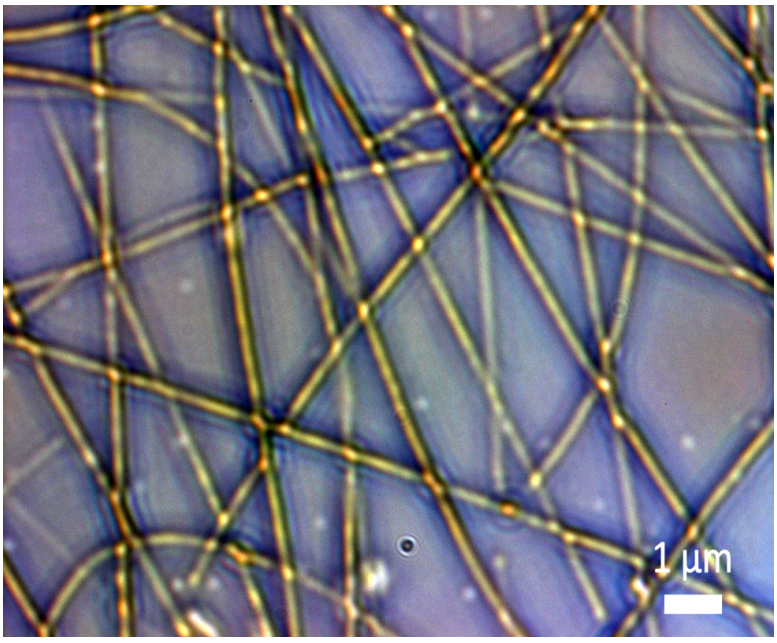

Figure II-4. Optical microscope (made by Zeiss Axiocam) image of PVP (1300K) – TA complex fibers.

The optical microscope magnifies the image with the help of the combination of glass lenses (Figure II-4 shows magnified image of nanofibers). A beam of light is sent through the object and the condenser lens focus the light ray on an object and objective lenses magnify the

beam of light. The objective lens can have a magnification of 10x, 40x …3000x.[43] Optical microscopy has a number of advantages such as the sample preparation is minimal and sample can be observed under atmospheric pressure and temperature. It doesn't need to be dried. Also, it is advantageous to use optical microscopy for the in-situ analysis which requires certain physiological conditions such as aqueous media.

Unfortunately, optical microscope can go only up to 3000x. This limitation of inadequate resolution restricts optical microscopy to observe any details at nanoscale. There are reports of using an optical microscopy for understanding the production process of nanofibers.[43, 44]

Scanning Electron Microscopy (SEM)

In Scanning Electron Microscopy (SEM), a finely focused electron beam is incident across the surface of the sample and the response of electrons is recorded. Interactions of electrons with sample can be categorized as secondary electrons, backscattered electrons and characteristic X-rays. These interactions are collectively called as signals and are collected by detectors to generate an image of the sample. Many factors such as electron energy, sample density, atomic number of an element and the topography of sample surface can affect the interaction of electrons.

To be able to perform SEM properly, sample needs to be conductive towards electron. So, to avoid repulsive reaction of electron beam on non-conductive samples surface, it is usually coated with thin layer of gold.

Generally, the advantages of using SEM includes high depth of sharpness, very high-resolution providing information about structures at various distances and angle. But on the other hand, SEM needs to be done under a vacuum. This aspect represents a drawback especially where there is requirement of wet conditions. This disadvantage is partly solved by using a low vacuum during SEM. Techniques like environmental scanning electron microscopy (ESEM) and aquaSEM

techniques can be performed under the aqueous conditions and enable the observation of samples in wet state.

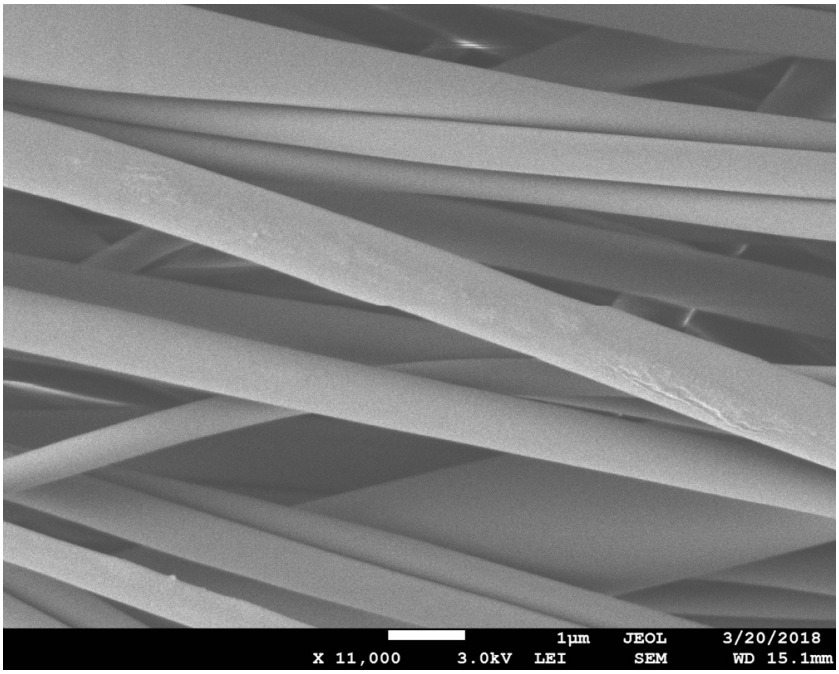

Figure II-5. Representation of a SEM microgram of electrospun nanofibers of PVP (1300K) – TA complex.

SEM and transmission electron microscopy (TEM) were found to be essential for investigation of nanofibrous materials with advanced structures as shown in Figure II-5. For example, core-shell structure obtained by coaxial electrospinning, the nano-coil structures formed during side-by-side and off-centered coaxial electrospinning and the influence of electrospinning conditions on the formation of such structures can also be investigated by these techniques.[16, 19, 26]

Atomic Force Microscopy (AFM)

Atomic Force Microscopy (AFM) measure the forces between a micrometer- scale cantilever with a sharp tip (diameter ~ 10-50 nm) and a sample. The tip is brought very close to a surface (scales in nm) to do a scanning over the sample. Attractive and repulsive forces resulting

from interactions between the tip and the surface will cause a positive or negative bending of the cantilever. The three-dimensional model of sample surface is reconstructed from individual positions of the tip.

This method gives information about the morphology and mechanical properties of the fibers such as modulus and hardness.[45] Compared to electron microscopy techniques, AFM can operate in nonvacuum environment or in wet condition such as in water or various organic solvents.[46]

Mechanical Characterization: Tensile Testing

There are many methods which are used to analyze mechanical properties of nanofiber. Conventionally, nanofiber membrane which are uniaxially spun are used to perform mechanical characterization due to its ease of testing.[25] Moreover, several groups have measure tensile properties of fibers using conventional testing method which is the testing of as-spun fiber mat

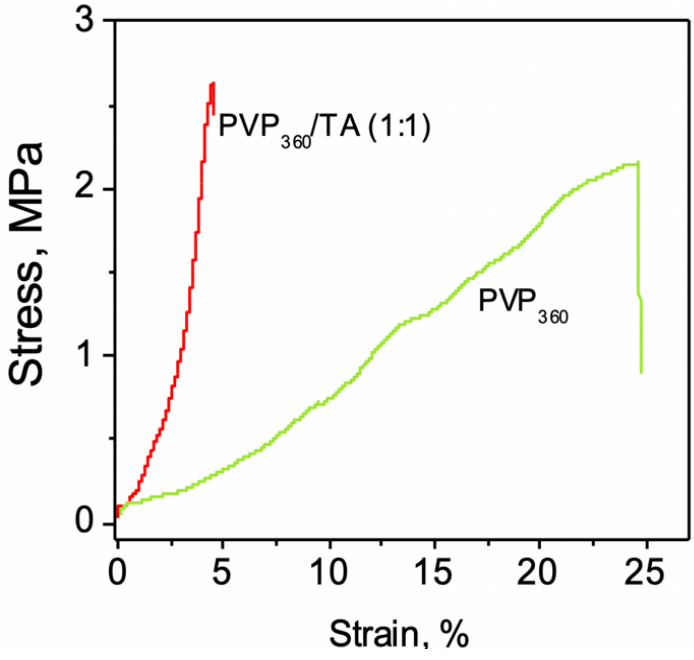

Figure II-6. Stress vs. strain curve of a nanofiber mat of PVP (360k)-TA complex spun at equimolar ratio.

with highly uniaxially oriented nanofibers. However, this technique is not applicable for measuring individual fiber mechanical. An example of stress *vs.* strain curve is shown in Figure II-6.

The overall mechanical properties of nanofibers mat are a function of the mechanical properties of individual fibers and the orientation of fibers within the mat. In last few years, some interesting characterization methods have arisen in order to characterize a single fiber to analyze nanomechanics of nanofibers.[47-50] Ding *et al*. used this technique to investigate the elastic modulus of a boron nanowires.[51] They clamped each end of a single nanowire to the tip of a soft and a rigid cantilever which were positioned parallel to one another but with opposite orientation, as shown in Figure II-7 (A). A piezoelectric bender was then used to gradually pull the soft cantilever away from the rigid one to stretch the nanowire until fracture. The stress *vs.* strain behavior was determined from the length of the nanowire which was frequently measured using a series of images that were taken during tensile loading, and the applied tensile force which was determined from the cantilever's deflection and its spring constant.[51] In a similar study, Zussman *et al*. mounted one end of an electrospun nylon-6,6 nanofiber to a stainless-steel wire and pulled the other end which was attached to a cantilever tip,[52] as illustrated in Figure II-7 (B). The deflection of the cantilever and the elongation of the nanofiber were monitored using a microscope, and the stress-strain curve was obtained to determine the Young's modulus and mechanical strength of the nanofibers.[52] Baker *et al*. anchored a nanofiber in lateral position with the help of optical adhesive to the ridges on the striated substrate as shown in Figure II-7 (C). Individual fibers were stretched laterally by moving cantilever tip between adjacent ridges. The lateral force applied to the fiber is measured by the torsion of the cantilever given by the deflection of a laser beam reflected off of the back of the cantilever.[53] The modulus, extensibility, elastic limit, and relaxation times of these fibers are measured and a molecular mechanism is proposed to account for these properties. These

results are then compared to measurements of other fibers that have been measured using the same technique.[54] The disadvantage of these cantilever-based tensile testing techniques is that they are time consuming and difficult to manipulate single fibers.

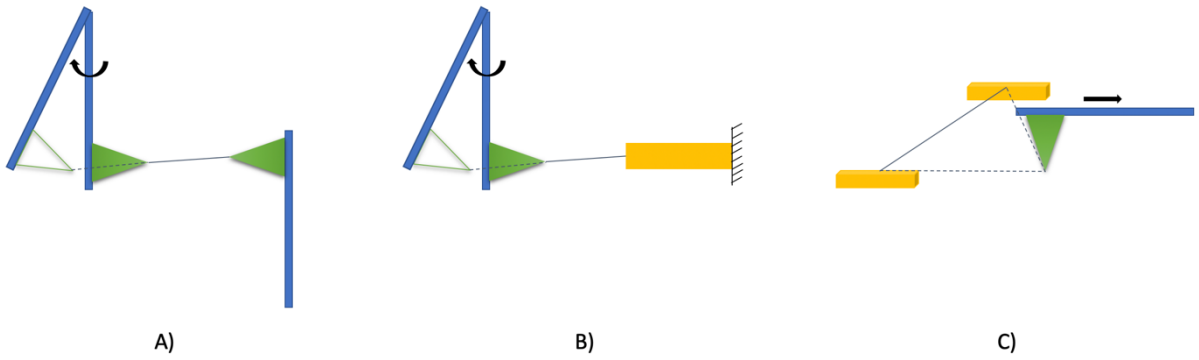

Figure II-7. Schematic representation of a mechanical testing of fibers using an AFM cantilever in which a) fiber is attached to the tip of soft and rigid cantilever b) fiber is attached to stainless steel wire c) fiber anchored in a lateral position with the help of optical adhesive to the ridges on the striated substrate.

CHAPTER III

INTRODUCTION TO RESEARCH

Significance of Research

The motivation of this research lies in the uniqueness of the properties of hydrogen bonded fibers. Very few reports of such fiber system exist with very little focus on hydrogen bonding system. Also, most applications in biomedical field, filtration systems or food industries require water-stable nanofiber mat to be able to withstand during operating process to withstand neutral pH conditions. Commonly available water-soluble mats need an additional step of chemical crosslinking to be able to preserve the fiber morphology in aqueous solutions as well as enhance the thermal and mechanical properties.[55, 56]

Hydrogen bonding is a convenient and powerful approach to crosslink, can occur between proton accepting group of non-ionic polymer and protonated carboxylic groups of poly(carboxylic acid).[5] Multilayer hydrogen bonded films are being extensively explored by our group as well as the others.[57-64] It has been previously showed that the hydrogen- bonded IPC between these polymers can simply be formed just by mixing interacting polymers together in common solvent.[65] These hydrogen-bonded interpolymer complexes (IPCs) possess mechanical and thermal properties which are entirely different from parent polymers.[66] The assembly method employed to prepare hydrogen-bonded complexes can largely impact their tunable properties. The layer-by-layer (LbL) method, in which sequential adsorption and deposition of hydrogen donor and acceptor component occur, provides a unique combination of the hydrogen-bonded complex properties due to the cross-linked nature of the thin multilayer assembly.[61, 67] This method can be applied on different surfaces and supports addition of a variety of materials or different polymers to the assembly.

Tannic acid, as a water-soluble natural polyphenol has been extensively studied in hydrogen-bonded LbL assemblies because of its excellent hydrogen donor phenolic groups.[67, 68] Tannic acid is especially attractive because of its diverse biological properties including antienzymatic, anticarcinogenic and antioxidant.[69-71] Mixing tannic acid with non-ionic polymers such as polyvinylpyrrolinone (PVP) and poly(ethylene oxide) (PEO) in water solutions often results in a phase separation and formation of IPCs.[68] The formation of such complexes is affected by many factors, including polymer molecular weight, concentration and pH. Previous work by Eral-Unal *et al*. showed that hydrogen-bonded multilayers containing PVP with TA are stable up to pH 8.5.[68] Despite its unique and interesting properties, nanofiber assembly of IPC-based systems are not widely explored yet. Only few examples come from Boas *et al.* and Meng *et al*., who demonstrated electrospinning fibers from polyelectrolyte complexes using electrostatic interactions.[72, 73] Apart from electrospinning of fibers containing polyelectrolyte complex, Boas et al. also explored dependency of stability of fibers on the pH of aqueous solution.[73] Here, we embarked on the investigation of hydrogen-bonded systems. Though the stimuli-responsive behavior of polymeric films has been reported extensively, to the best of our knowledge, our group is the first to create nanofibers out of hydrogen-bonded system via electrospinning that exhibits pH-responsive behavior and antioxidant properties.

Here, it is been demonstrated that solid fibers can be electrospun from hydrogen-bonded complex system of PVP – TA. Chemically and thermally robust fiber mats can be formed using an extremely broad range of electrospinning parameters, including various concentrations and mole fractions of components. Electrospinning of hydrogen-bonded complex based materials has tremendous potential for use in applications, such as wound healing, water remediation, catalysis. However, to fully realize the potential of these materials, key fundamental questions regarding the

underlying physics and limitations of this approach must be addressed, particularly with regards to the effect of polymer molecular weight and other molecular level details on the thermodynamic and kinetic behavior of the system.

Research Objective

The objective of this research was to explore electrospinning of hydrogen-bonded nanofibers as function of component ratios and molecular weights, investigate the effect of hydrogen-bonding on mechanical properties and evaluate pH stability and antioxidant ability of a fiber mat. The research progressed in two separate phases. Phase one (Chapter 4) was to electrospun the nanofiber mesh, determine the appropriate electrospinning parameters, characterize nanofibers using thermal and optical characterization techniques determine the pH stability in various pH environment and antioxidant ability of a fiber mat. Phase two (Chapter 5) was to conduct a mechanical testing of a fiber mat to explore the effect of hydrogen bonding on mechanical properties of the fibers.

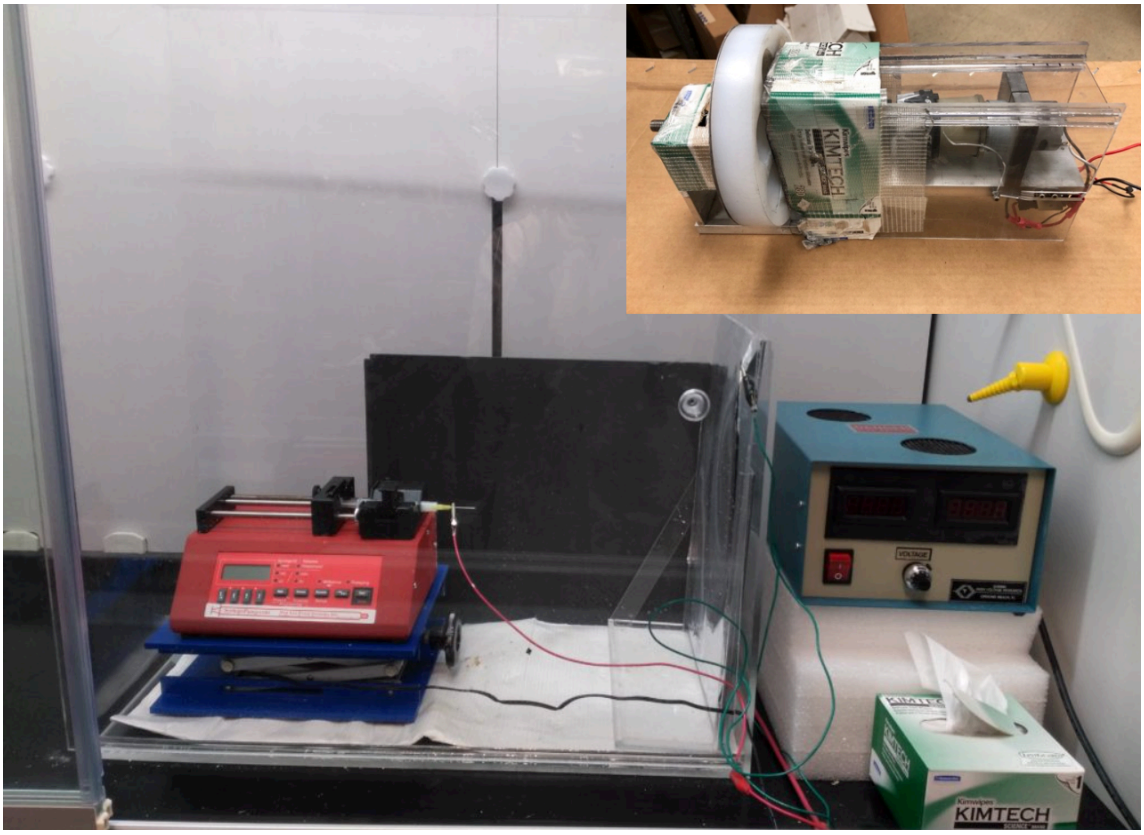

Figure III-1. Electrospinning setup showing an active electrospinning process on a flat plate collector was used for all the experiments. Inset image shows the rotary collector which was used to spun uniaxially aligned fibers.

Phase one included setting up the electrospinning apparatus and altering different parameters to get consistent fiber formation or fibers without beds.

For spinning uniaxially aligned nanofibers an electrospinning platform with rotary spinner were created. The main components can be seen in Figure III-1. They include 1) a Plexiglas box, 2) a high voltage power supply, 3) a syringe pump, 4) a ground plate collector, 5) dispensing needle, and 6) a needle height adjusting knob 7) Rotary collector (inset image). The adjustable parameters included voltage, needle to ground plate distance, flow rate, and solution concentration. During this phase, all of these parameters were altered in order to get the most consistent fiber

formation possible. In particular, solution concentration was studied to get a solution that would have the longest working time, without becoming too viscous to spin properly. Differential scanning calorimetry (DSC) and morphological analysis of nanofibers was done using SEM. pH stability of fibers at pH values of 2, 6 and 10 was also tested and antioxidant properties of a fiber mat and eluted TA from a fiber mat was examined.

Phase two consisted of mechanical testing of nanofibers to assess the integrity of fibers. In this process, the nanofiber mesh was tested under mechanical load in a dry ambient condition (24^{o}C and 50-60 % RH) to determine the strength of nanofibers. In order to be used in the particular application such as filtration or biomedical application, the mat needs to be mechanically robust and shouldn't break under an ordinary stress.

CHAPTER IV

ELECTROSPINNING HYDROGEN BONDED COMPLEX FIBERS

Introduction

Electrospinning process has been recognized as a powerful single-step assembly technique to fabricate nanofibers by electrostatic forces.[74] This unique technique has the potential to prepare free-standing polymer mats with novel and advanced properties. Electrospinning can produce fibers with a diameter of scale in nanometer from a wide range of polymers and is a technique with renewed interest and development in the last decade.[24] Aforementioned exceptional properties make nanofibers appealing candidates for a variety of applications such as water purification[17, 75-77], biomedical related research in tissue engineering[16, 78-82] as well as wound dressing.[14, 83-86]

Inspired by LbL hydrogen bonded systems the goal was to produce robust nanofibers out of the same system. Hydrogen bonds are a good example of interactions that can sustain elevated ionic strength of solutions and are stable for a wide range of pH. Ability to control stability and mechanical integrity in a range of pH is crucial for biomedical application of the systems. In addition, a stoichiometry should play an important role. The number of components that possibly can form HB pairs allow a variety of functionalities and compositions including small molecules, polymers, and inorganic species.

Electrospinning Apparatus

The electrospinning apparatus used for these experiments consists of Plexiglass box, a high voltage power supply, syringe pump, rotary collector attached to the ground connector, flat plate collector attached to the ground, spinneret with flow control mechanism, syringe attached with 21L sized needle. The apparatus can be modified to electrospun any desired polymer solution with

spannable viscosity and surface tension by adjusting the apparatus parameter and in any desired orientation i.e. either uniaxially oriented or randomly orientated fibers.

The main component of the electrospinning process is the plexiglass shield box seen in Figure III-1. It is designed to house a rotary collector (inset image of Figure III-1) and spinneret. It also separates the highly charged electrospinning area from the outside world. The design also minimizes air flow irregularities that could disturb nanofiber formation or disrupt the electric field. The high voltage power supply (ES 30-0.1P, Gamma High Voltage Research) has a maximum voltage output of 25 kV and 1.5 mA current. The high voltage power supply is attached to the needle tip and to the ground collector plate to complete the circuit.

A flow rate was controlled by a syringe pump (NE-1000, New Era Systems, Inc.) which can vary flow rates between 0 and 99 ml/hr. The syringe holding the polymer solution is inserted into the pump system. The ground plate collector and dispensing needle are both located inside of the Plexiglas box so they can be separated from the outside environment and attached to an electrode from the voltage power supply. There is a Plexiglas base that lifts the ground collecting plate so the proper separation distance can be achieved. The ground pate is attached to the other electrode from the voltage supply.

Materials and Methods

Electrospinning Solution Parameters

The solution parameters which determine whether solution can be electrospun are its viscosity and surface tension. These are dependent on the polymer that is selected and its concentration in the solvent. The interacting polymers were pre-selected polymers for this experiment. The variables that could be altered were the polymer concentrations, the solvents, and the solvent ratios. Polyvinylpyrrolidone (PVP) (Mw = 1,300,000 and 360,000), and dimethyl

sulfoxide (DMSO) were purchased from Alfa Aesar. Tannic acid (TA), PVP (Mw = 55,000) and N, N- dimethylformamide (DMF) were purchased from Sigma Aldrich.

Three separate sets of the fibers were made for different studies. The first set was used for investigation of the effect of solids concentration in spinning solution on the diameter of the fibers. In this case, homogeneous solutions of PVP/TA were prepared in 75/25 DMF/DMSO (v/v) mixture by adding PVP and TA at equimolar ratio of hydrogen bonding units but varied total 6 concentration of solids (10.5-15 wt.%) with gentle stirring at ambient temperature overnight. The second set of fibers was with varying amounts of mol fractions of TA by repeating units to study the effect of fraction of components on mechanical properties an antioxidant property of fibers. In this case, PVP (1300k) and TA were dissolved in the same solvent mixture as the first set at 13.5 wt.% total concentration of solids, but varying the mole fractions of TA to PVP. In third set of fibers an equimolar ration of PVP/TA fibers were spun and molecular weight of PVP was varied as 55kDa, 360kDa and 1300kDa. Third set of fibers also include a control set of experiment in which fibers of pristine PVP's (molecular weights – 55k, 360k and 1300k) were prepare for a comparison study. All solutions were used for electrospinning immediately after preparation.

Electrospinning Parameters

Once the different solution parameters are selected, fiber formation is dependent on the proper selection of the apparatus parameters. Parameters such as voltage, plate separation distance, flow rate, and needle gauge all have drastic effects on fiber formation. They are all interdependent and must be optimized to generate the most uniform fiber mesh. The flow rate (μ) was controlled by a syringe pump (New Era pump, NE-1000) and kept constant (10 μL/hr). A voltage (V) in the range of 11– 18 kV (Gamma high voltage) were applied depending upon the type of solution spinning. A rotatory wheel, with 1000 rpm was placed at the distance (d) of 35 cm from the

spinneret (needle 21G) to collect the aligned fibers. The final nanofiber mat was easily collected from the aluminum foil and kept under the hood to remove any residual solvents. The nanofiber films were used to make specimens for mechanical testing.

A summary of these parameters can be seen in Figure IV-1. These were then altered as needed to generate the most uniform scaffold. Aluminum foil was selected as the ground plate collector, because it is conductive, inexpensive, and pliable. Pliability was important because it would allow the scaffolds to be easily removed from the metal surface by peeling the foil away

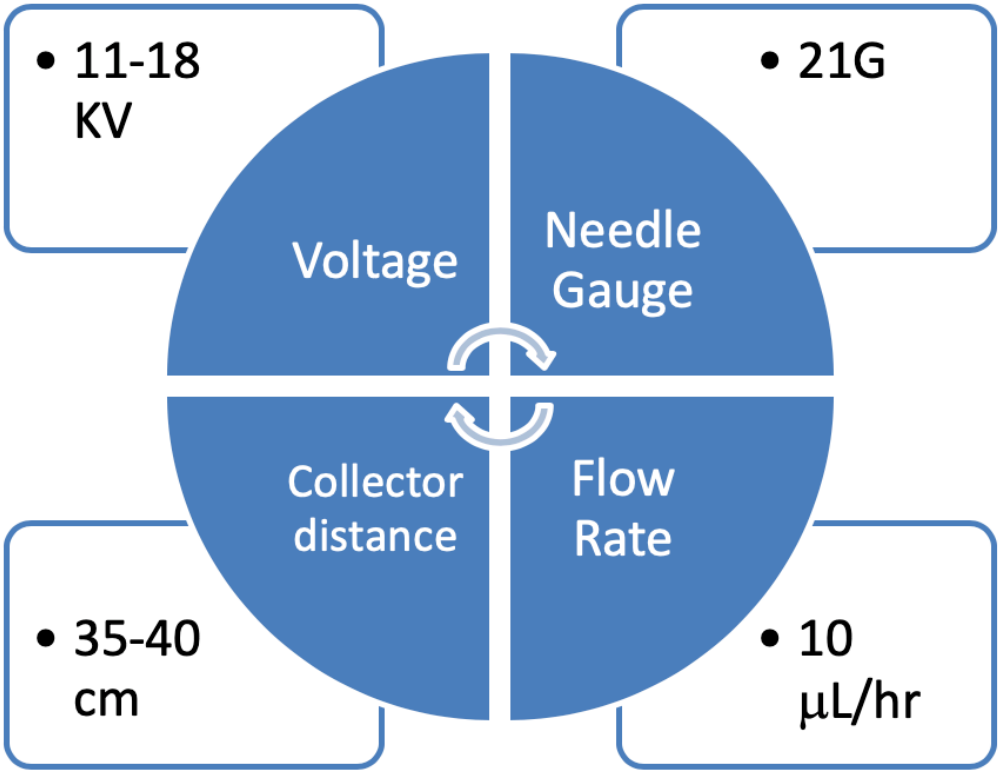

Figure IV-1. Electrospinning working parameters used for all the experiments.

from the scaffold. Other thicker metal plates like copper could also be used, but it would have been more difficult to remove the scaffolds and could have resulted in mesh defects or deformation.

Challenges in Electrospinning Process

The biggest challenge in the electrospinning process was making a solution that could be electrospun. The molecular weight of the PVP is varied from 55k to 1300K. Lower molecular weight polymer complex are easier to spin due to lower viscosity but higher molecular weight polymer complex makes the solution very viscous and difficult to spin at high concentrations.

High molecular weight polymers have longer monomer chains and thus an increased amount of chain entanglement which makes it more viscous. The problem is compounded when the polymer needs to be dissolved in a solvent solution that evaporates quickly. Solvents such as DMF and DMSO does not evaporate readily and does spare some time in the preparation as compared with ethanol or other alcohol.

In addition, higher molecular weight PVP did not dissolve readily in the solvent solution. To overcome this problem, the higher molecular weight PVP and TA was added with combination of DMF and DMSO at least 12 hours before electrospinning. This would allow it to dissolve properly.

Maintaining the ideal combination of solvents for each combination proved to be difficult, as each polymer combination had different component ratios. So, the solvent combinations were needed to be optimized in order to obtain bead free fibers. DMSO has very high boiling point compared to DMF and also very hard to get rid of it from the fibers. So, maintaining the lowest possible required amount of DMSO to dissolve the polymer in DMF was challenging.

There were additional problems associated with humidity and temperature in the laboratory. The electrospinning is influenced by the environment in the room. In order to prevent nanofiber alterations due to environmental parameters, the electrospinning set-up was set up in a

fume hood. By placing the setup in the fume-hood, not only the environmental parameters were controlled but the fumes of solvents evaporated during the spinning process were also contained.

Fiber Mesh Analysis Using SEM

After the complex nanofiber meshes were created, a scanning electron microscope (SEM) was utilized to acquire detailed images of the nanofiber scaffolds. These images are valuable to demonstrate that a uniform and uniaxially orientated nanofiber mesh is created. Based on the fiber deposition from the images, polymer concentration changes can be made to improve the fiber deposition. The fiber morphology was observed with a scanning electron microscope (SEM) JEOL JSM-7500F equipped with a cold cathode UHV field emission conical anode gun. The images were taken at the probe current of 10 μA and 3 kV accelerating voltage. The surface of the samples was sputtered with 2 nm Pt/Pd coating to avoid charging.

The SEM can be adjusted in several ways to obtain the clearest image. Secondary electron detection is the most common setting and collects low energy electrons from the sample surface. This detection method is capable of high depth images where the electrons hit the surface and are ejected towards the collector. Backscatter electron imaging consists of high energy electrons that originate in the electron beam, hit the sample, and are reflected back. This detection method allows more surface detail, but has less image depth. Both methods were adjusted to view the samples at different magnifications so that the most detailed images were collected.

Morphological and Statistical Analysis of Nanofiber Mesh

Morphological analysis of the fiber mesh was performed using image processing software called ImageJ software. This software was used to analyze the nanofiber diameter data from different SEM images. This data is useful to verify that nanofibers are being generated as well as to validate consistency of the mesh diameter. All the data was imported in OriginLab® software

and plotted and the mean, standard deviations and histograms can all be graphically represented to better visualize the data that was obtained.

Thermal Properties of Nanofibers Using DSC

TA Instruments Q2500 differential scanning calorimetry (DSC) was used to perform thermal analysis on the fibers. All experiments were carried out using a 10^{o}C/min heating and cooling rates. Samples were prepared by placing 10–12 mg of nanofibers into hermetically sealed aluminum pans. Glass transition temperature (T_g) was found through the step in DSC profile using thermal analysis software.

The pH Stability of a Fiber Mesh

Stability of the fiber mats at different pH was studied with UV-vis spectrophotometer (UV2600, Shimadzu Inc.) by measuring the intensity of the absorbance peak of the releasing tannic acid. The samples were cut into small pieces, weighted, and placed into 20 mL of DI water at pH 2, 6, and 10. After certain periods of time, 1 mL of the extract was mixed with 2 mL of DI water and measured in the range of the wavelength 190-600 nm, using DI water as a reference. The amount of released tannic acid was calculated as a percent of the tannic acid in solution to the total amount of tannic acid used for fibers production. The amount of tannic acid in the solution was calculated using absorbance of tannic acid at 270 nm at pH 2, 280 nm at pH 6, and 340 nm at pH 10, and corresponding coefficient of extinction. The coefficients of extinction at different pH were independently determined by measuring absorbance of TA solutions of known concentrations at various pH.

Antioxidant Activity of a Fiber Mesh

Antioxidant activity of the fibers was evaluated as the ability to reduce ABTS radicals. To make ABTS radicals, equal volumes of ABTS precursor and potassium peroxydisulfate solutions

with concentrations of 7 mM and 2.45 mM in DI water, respectively, were mixed and left in the dark overnight to react.[87] This solution was further diluted with DI water to achieve desired absorbance at 730 nm. Small pieces of the fiber mats with the mass of 1 mg were immersed in 50 mL of ABTS solutions. After different periods of time, 1 mL aliquots of the solutions were taken and diluted with 2 mL of DI water and analyzed using UV-vis. The antioxidant activity was calculated as a decrease in intensity of the ABTS absorption peak at 730 nm. To account for contribution of TA released to solution, a separate set of the experiments was conducted in which pieces of the fibers were placed in 20 mL of DI water and 50 µL aliquots of the supernatant were collected after certain periods of time. The aliquots were added to 2.5 mL of ABTS solution and left for 1 week to assure completion of the reaction. The absorbance of solutions at 730 nm was used to calculate the antioxidant activity of TA released from fiber mats. The antioxidant activities of the fiber mats and the extracts were quantified as the moles of ABTS reduced per 1 mg of the fiber mats.

Results and Discussion

Electrospinning of Nanofibers

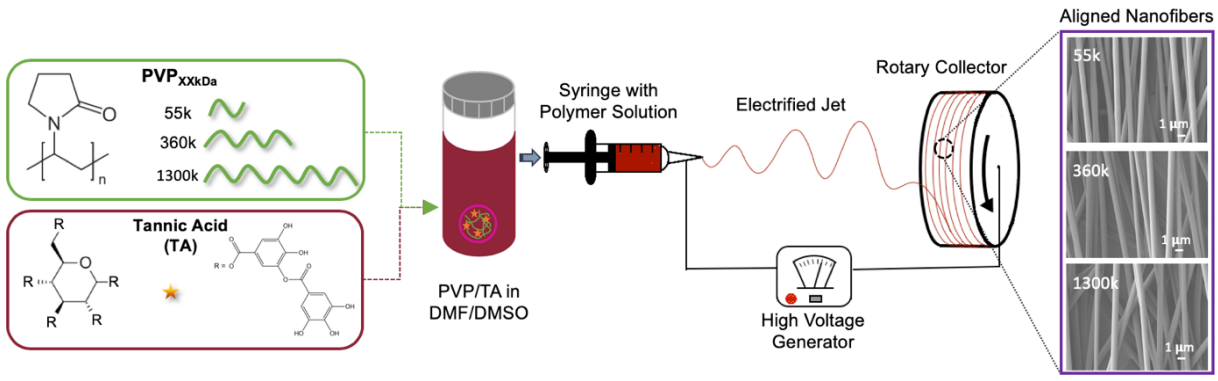

Figure IV-2. Schematic representation of electrospinning of PVP-TA fibers from DMF/DMSO solutions. The scanning electron microscope (SEM) micrograph shows as-spun free-standing fibers electrospun from a 13.5% PVP-TA solution containing the equimolar ratio of hydrogen bonding partners.

Electrospinning was performed using a mixture PVP/TA in an organic solvent. A schematic of an overall procedure is shown in Figure IV-2. Electrospinning of PVP/TA IPCs from aqueous solutions was not possible due to clogging of the needle by solid precipitates. A strategy of disruption of hydrogen bonds between PVP and TA in electrospinning solutions was then pursued. In contrast to electrostatically associated PECs which can be 'soften' by disruption of ionic pairing by inorganic salts,[72] hydrogen-bonded IPCs are not significantly affected by the addition of small ions. However, low-molecular-weight acceptors of hydrogen bonds, such as DMF and DMSO, are capable of modulating interpolymer hydrogen bonding.[88, 89] Mixing pf PVP and TA in DMF lead to hydrogen-bonded coacervates, in which binding between PVP and TA was partially disrupted. To allow for a facile control of fiber composition and unified processability of solutions with widely varied PVP-TA ratios, we were seeking for a solvent which completely dissociates PVA-TA hydrogen bonding. Based on a recent finding that DMSO serves as a very strong competitor for disrupting polymer-polymer interactions we used DMF/DMSO 75/25 (v/v) mixture as a solvent. DMSO molecules efficiently competed with PVP for hydrogen bonding with TA, preventing formation of hydrogen-bonds. As a result, PVP/TA solutions were clear viscous liquids, which could be easily fed through the needle. At the same time, hydrogen bonding between PVP and TA occurred during the spinning process, as solvent evaporated. The fiber compositions, controlled by the ratio of the components in the spinning solutions, are abbreviated as PVP (Yk)-TA_X, where X is the molar fraction of TA hydrogen-bonding units, calculated as the ratio of moles of hydroxyl groups of TA, to the sum of moles of PVP repeating units and moles of hydroxyl groups of TA and Y is the molecular weight of PVP used. For e.g. fibers abbreviated as PVP (1300k)-$TA_{0.5}$ contain equimolar numbers of PVP of molecular weight of 1300 kDa and TA hydrogen-bonding units. Figure IV-2 depicts the procedure used for electrospinning of PVP-TA

During fibers production on a collector, a rotating mandrel covered with the conductive aluminum surface was used (Figure IV-2). After deposition, nanofibers were easily detached from the surface in a form of mats. Formation of fibers on a rotating mandrel allows to produce aligned uniaxial fibers and this approach was used previously.[24] The surface and diameter distribution of resulting fibers were studied with SEM. In all analyzed samples quantification was based on multiple SEM images taken at random spots.

Morphological and Statistical Analysis of Nanofiber Mesh

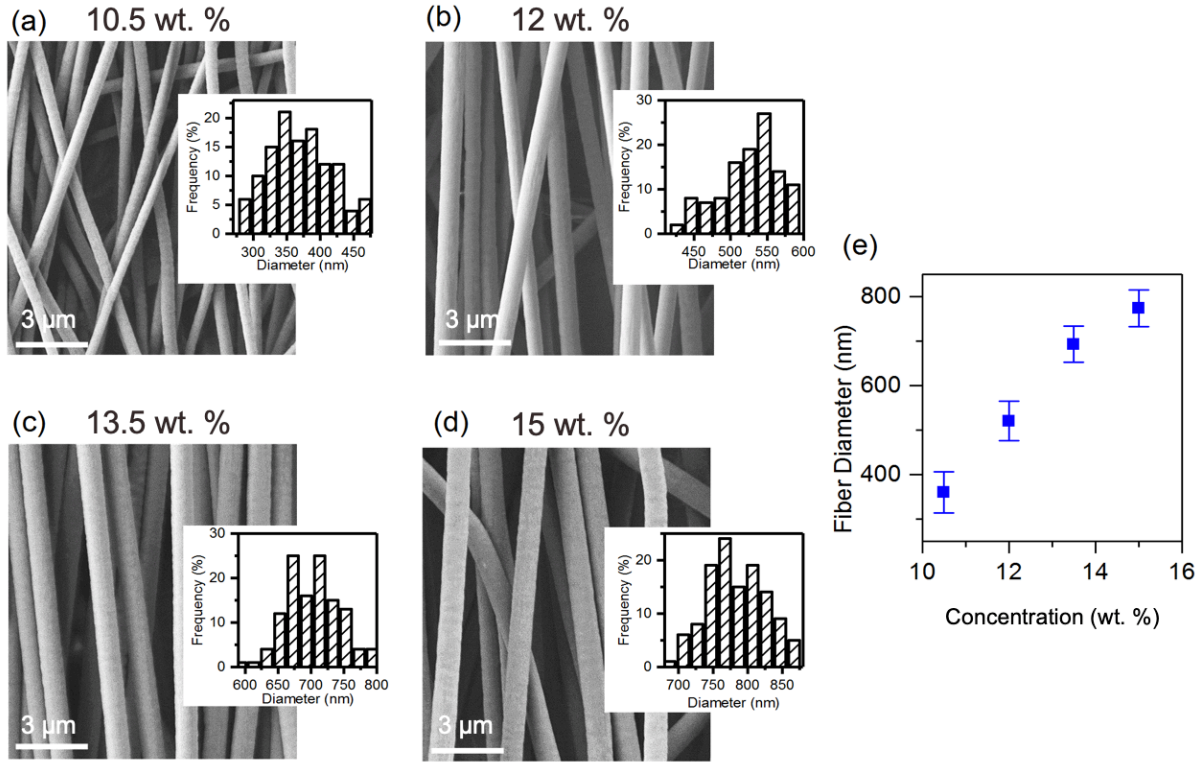

Figure IV-3. Variation of fiber diameter as a function of concentration of a solution containing PVP (1300k) - TA at equimolar ratio a) 10.5 wt.% b) 12 wt.% c) 13.5 wt.% d) 15 wt.%.

The diameter of the fibers depends on the spinning parameters, including concentration of the solution (or its viscosity),[90] voltage, pressure, and distance between the needle and the

receiver.[39] The series of the fibers were spinned from the PVP (1300k) -TA solutions with different concentrations but equimolar composition to study the dependence of the fibers diameter on concentration. Consistent with multiple literature reports,[27, 39, 91] the fiber diameter was significantly dependent on solution concentration which is evident from Figure IV-3. The average

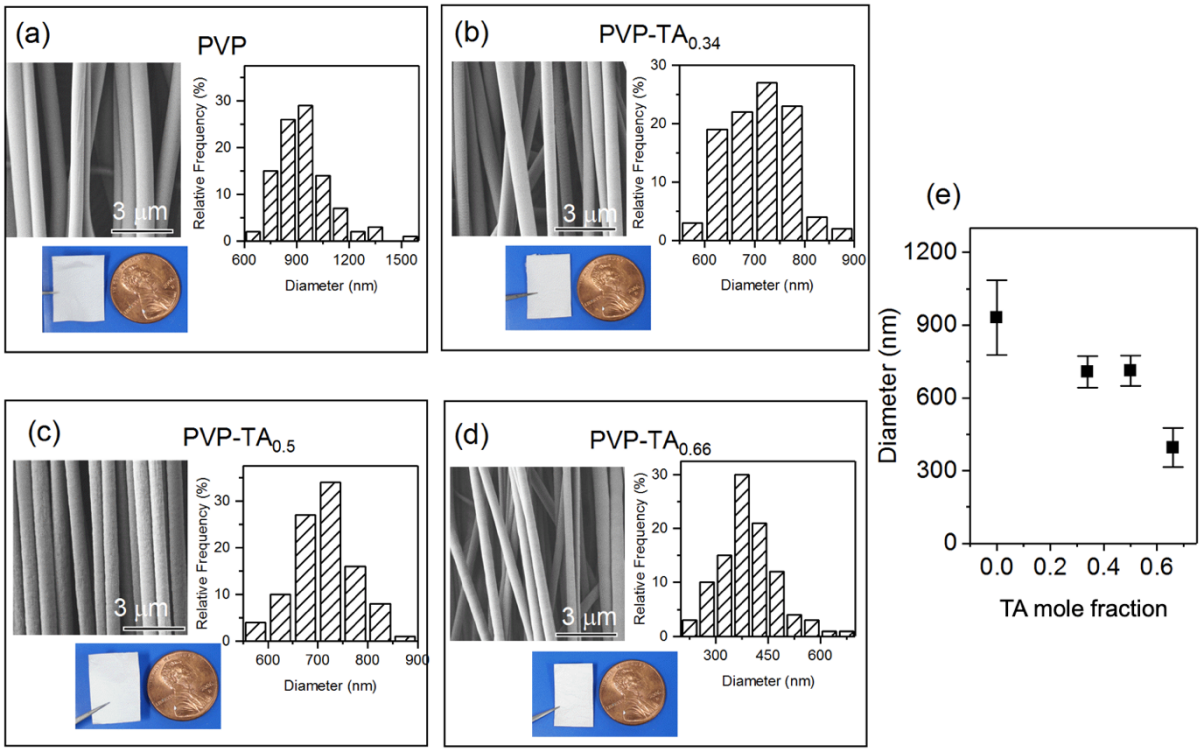

Figure IV-4. The dependence of the fiber diameter on the mole fraction of TA in PVP (1300k) - TA complex nanofiber a) Pristine PVP b) PVP-$TA_{0.34}$ c) PVP-$TA_{0.5}$ d) PVP-$TA_{0.66}$.

diameters and their distributions were calculated by analyzing at least 100 fibers represented by multiple SEM images. The fiber diameters had a were relatively uniform and increased from 360 to 773 nm when total concentration of PVP and TA in electrospinning solutions was raised from 10.5 wt. % to 15 wt. %, respectively. This effect is regularly observed in electrospinning, because more viscous solutions are harder to pull from the needle by an electric field.[27, 91]

The PVP-to-TA ratio in the fibers could be easily controlled by the mass ratio of components in the initial solutions and was expected to control the total number of hydrogen bond between PVP and TA, and therefore the mechanical properties and water-solubility of the fibers. Figure IV-4 summarizes SEM studies of the fiber diameters with varied PVP (1300k) -TA compositions prepared from solution with the fixed total concentration of 13.5 wt % in DMF/DMSO. It can be observed from the results that the average fiber diameter has decreased from to 700 nm for PVP-$TA_{0.33}$ to 350nm for PVP-$TA_{0.66}$ systems due to a decrease in the solution viscosity as the fraction of polymeric component in the mixture was decreased.

Thermal Properties of Nanofibers

TGA and DSC analysis of pristine components and complex fibers was performed to detect thermal stability of the components of the fibers and confirm the formation of the complex by

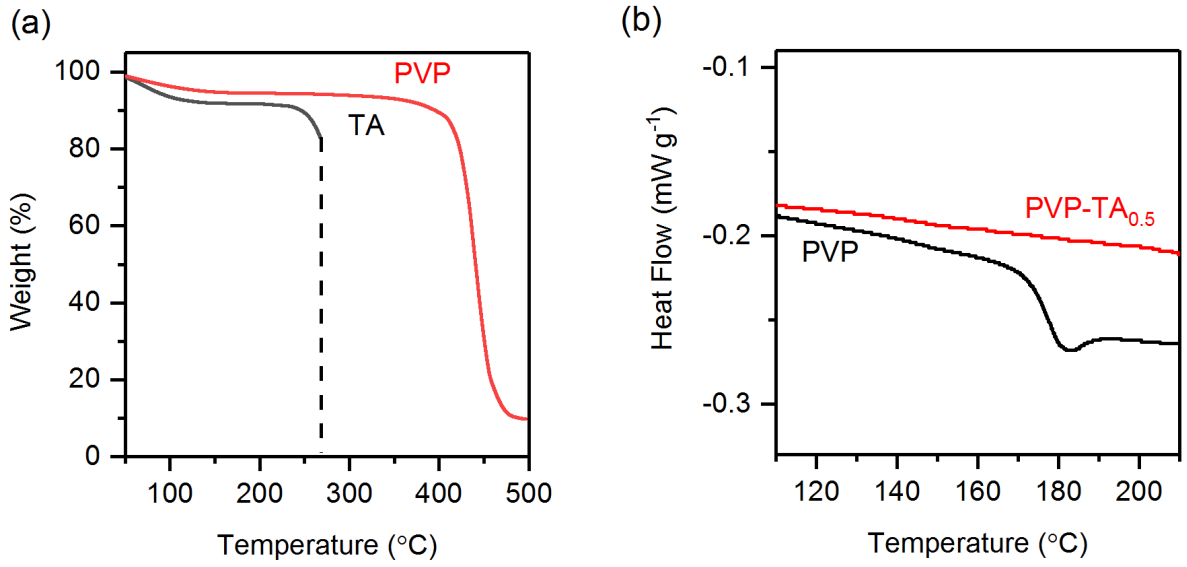

Figure IV-5. Analysis of the thermal properties of the pristine components and PVP-$TA_{0.5}$ fibers: a) Representative TGA profiles of pristine PVP (1300k) and TA; b) DSC thermograms of pristine PVP and PVP-$TA_{0.5}$ fibers.

determination of the changes in the glass transition temperature respectively. Figure IV-5 shows TGA and DSC results for the fibers made of PVP (1300k) -$TA_{0.5}$ and PVP (1300k). The TGA data show ~5-8% loss of water in both PVP (1300k) -$TA_{0.5}$ and pristine PVP fibers, yet a significant difference in the thermal stability of these molecules. Unlike PVP, which did not decompose to the volatile products up to temperature of ~400 °C, decomposition of TA started at ~230 °C, in agreement with its high chemical reactivity and lower molecular mass.[92] As shown in Figure IV-5, while glass transition temperature of 178 °C observed for PVP (1300k), PVP (1300k) - $TA_{0.5}$ complex did not exhibit temperature transitions in the range of temperatures between 110 and 225 °C (with the upper temperature determined by the decomposition temperature of TA), suggesting loss of segmental mobility PVP as a result of hydrogen bonding with TA.

TA starts decomposing at ~225 °C, which limits the temperature range for fiber mats application. Glass transition temperature was not observed for the fibers in the temperature range up to TA decomposition. This is indirect proof of the complex formation between TA and PVP in fibers. When PVP chains interact with TA, they lose their mobility and cannot go through the glass transition anymore.

pH Stability of Nanofibers

An important property that defines future applications of the fibers is their stability in aqueous solutions. Because individual PVP and TA components are readily soluble in water, but loose this capability after binding within a hydrogen-bonded complex, therefore it was important to study the effect of the fiber composition on their stability in aqueous solutions. To that end, the fibers were immersed in solutions at specific pH values for 50 days, and the amount of eluted from the fibers TA was measured by analyzing supernatant solutions by measuring their absorbance in the range of 257 to 278 nm. Figure IV-5 shows the SEM images of the fibers immersed in solutions

at pH 2, 6 and 10, along with the percentage of TA eluted from the fibers to the aqueous solutions after 50 days of immersion.

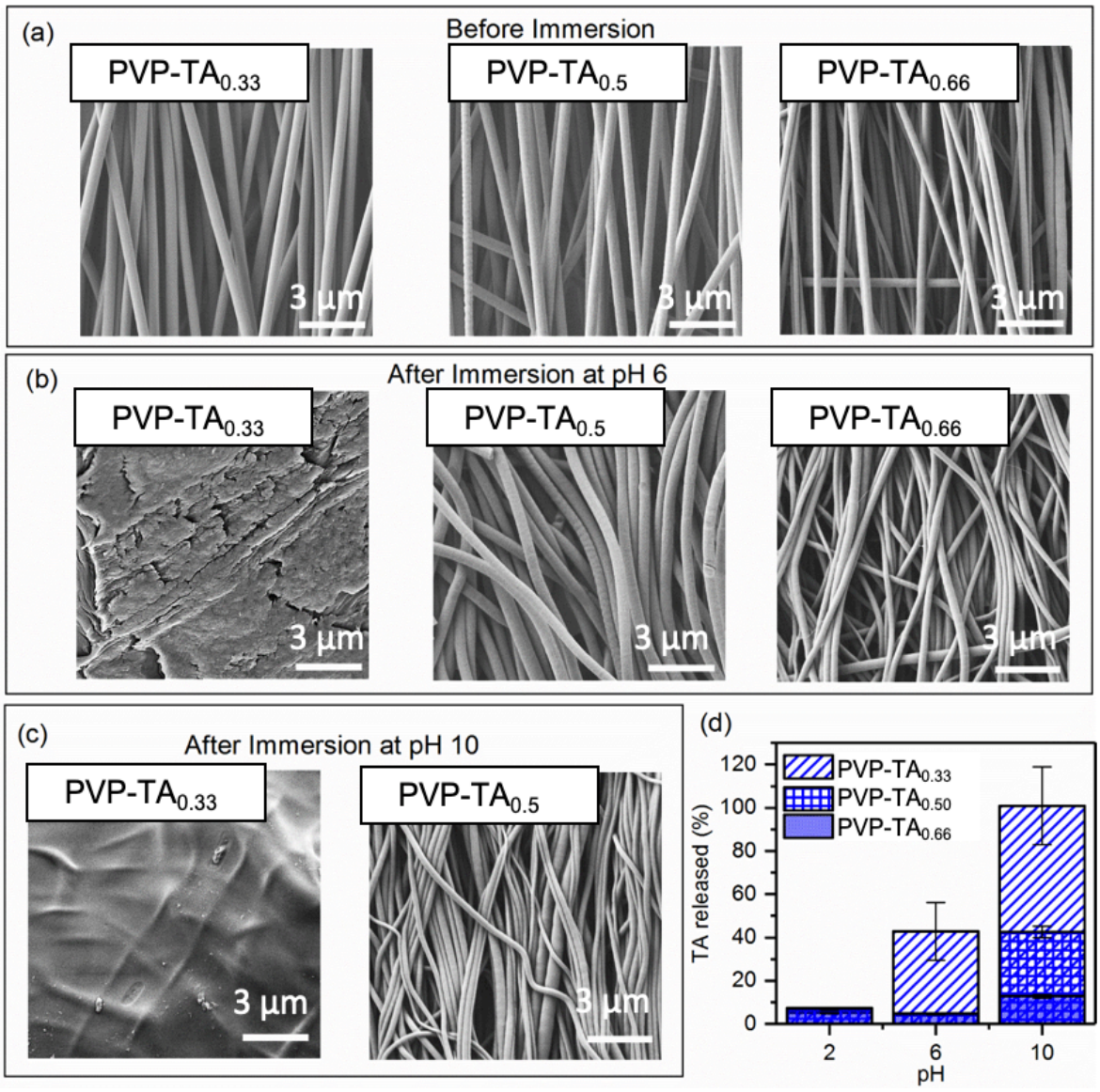

Figure IV-6. SEM images of fiber mats of PVP (1300k) – TA at various molar ratios of TA (a) before and (b) after 50 days of immersion at pH 6 and (c) pH 10 (d) The amount of eluted TA as a function of pH of the immersion solution.

All the fibers demonstrated high stability at pH 2, which is in agreement with the results reported for the stability of PVP-TA LbL films reported previously.[68, 93] Small amount of TA

released to solution (5-7%) at pH 2 was likely a result of the small number of non-stoichiometric TA molecules included within HBFs during spinning. The difference between the fibers with various PVP-to-TA ratios became more significant when the solution pH was raised, however. At pH 6, the fibers made with excess of PVP (PVP-$TA_{0.5}$), completely lost their morphology as shown in Figure IV-6 (b), and released 42.8±13.3 % of TA (Figure IV-6 (c)). At the same time, even though the fiber mat retained some integrity after 50 days of immersion, the fiber swelling and coalescence had occurred as suggested by the SEM images in Figure IV-6 (c). At pH 10, these fibers which contained excess of PVP fully dissolved after only one week of immersion (Figure IV-6(c)). In contrast, fiber mats made of the stoichiometric IPCs of PVP (1300k) and TA, as well as fibers containing excess of TA (PVP (1300k) -$TA_{0.66}$) demonstrated significantly higher stability at pH 6 and 10. At pH 6, the elution profiles for both compositions were similar, the amount of released TA not exceeding 4-5%. These fibers retain the morphology even after 50 days of immersion (Figure IV-7). At pH 10, fibers containing excess PVP completely dissolved, but as the

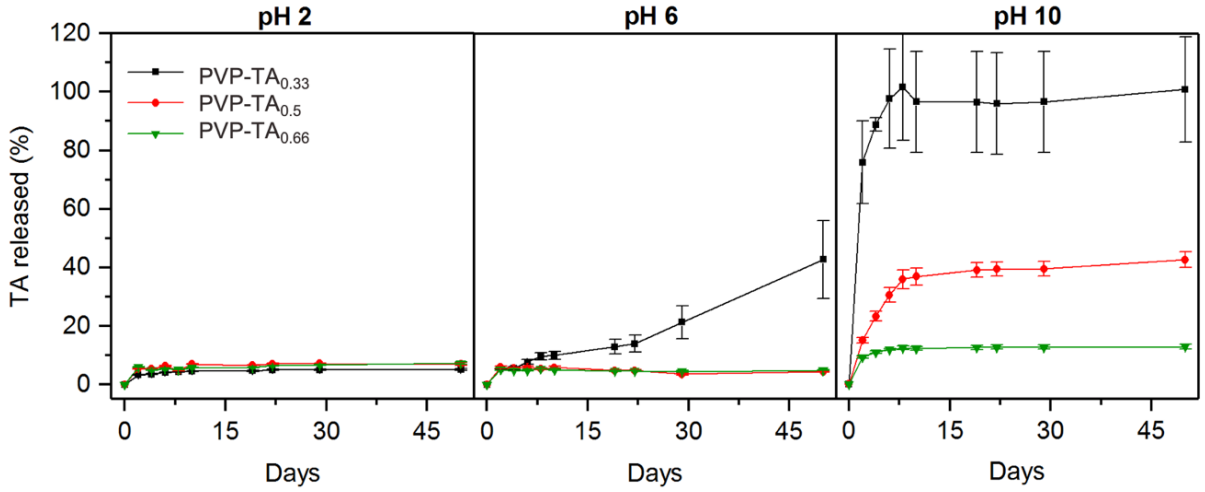

Figure IV-7. The profiles of the tannic acid release from fiber mats of PVP (1300k) – TA at various molar ratios of TA immersed in DI water at different pH for 50 days.

content of TA in the fibers was increased, the fibers re-gained their stability, releasing only ~18% TA at pH 10, and preserving their fibrous morphology. These results are consistent with our previous results on the stability of PVP-TA multilayers in a wide range of pH values, which is explained by the high ionization constant of TA (*pKa* ~8.5). The persistence of the network of hydrogen bonds between PVP and TA allow to retain fiber morphology in solutions at neutral pH values. Our results show that the effect of pH on fiber functionality, stability and morphology can be engineered at the fiber processing step by controlling the ratio between the hydrogen-bonding components. If PVP is taken in excess, fibers swell and even dissolve because of the deficiency in number of hydrogen bonds which stabilize the fibers in aqueous solutions, while the use of the higher mole fractions of TA allowed to obtain stable fibers. Our results also show that by controlling the composition of electrospun fibers allows one to engineer not only the fiber stability, but also the dose of TA released from solution in response to pH triggers.

Antioxidant Properties of Nanofibers

TA is a natural antioxidant whose antioxidant activity was mostly studied in solution when TA is readily available for the reaction with radical species.[94] Contrary to solution, TA assembled within fibers is less available for a reaction with dissolved radicals, which need to diffuse into the fibers to complete the reaction. Antioxidant activity of the fiber mats was assessed by standard ABST test, which quantified the capability of the mats to reduce ABTS radials in solution. To perform these experiments, coupons of the fibers made with different PVP-to-TA ratio of equal weight of 1 mg were exposed to 50 mL of ABTS radical solution, and the amount of the radicals reduced was measured at different time points during 50 days of immersion time. At the same centime, control experiments were designed to answer a question of whether the measured antiradical activity originated exclusively from the TA assembled with the fibers, or was a result

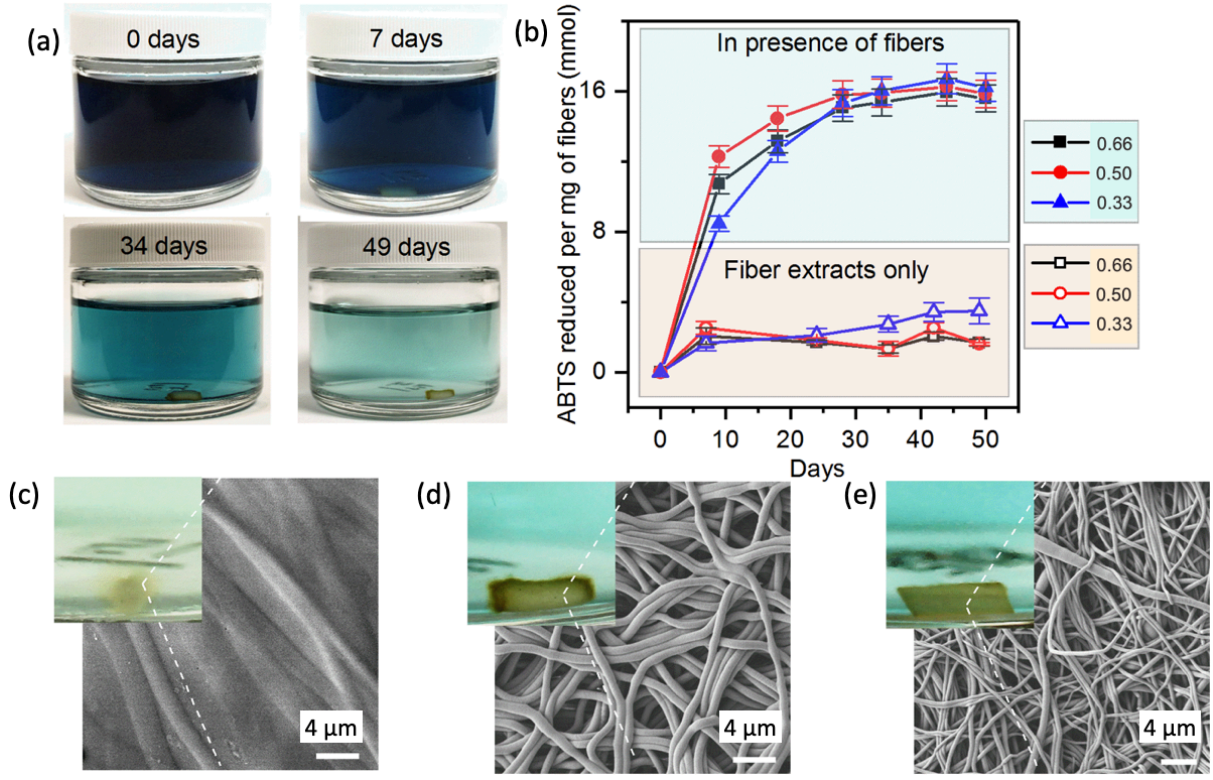

Figure IV-8. Digital images of PVP/TA fiber mats upon exposure to ABTS solution (a); Calculated amount of the reduced ABTS radical by fiber mats as well as fiber mats extracts (b); images of PVP (1300k) -$TA_{0.33}$ (c) and PVP (1300k) -$TA_{0.5}$ (d) and PVP (1300k) -$TA_{0.66}$.

of TA released from the fibers in the supernatant solution. In these experiments, fibers were immersed in DI water rather than ABTS, aliquots of the extracts were collected at specific time intervals and added to ABTS radical solution. Figure IV-8 (a) and (b) visualize changes in intensity of ABTS solutions after immersion of PVP-TA mats and summarize the results of antiradical activity studies with fibers of varied compositions.

The reduction profile suggests that while small amount of ABTS radicals were reduced by released tannic acid, the number of radicals reduced by fiber mats after 50 days of immersion is almost 10 times higher than the number of radicals reduced by eluted TA, which suggests that antioxidant activity of fiber mats comes mostly from fiber-assembled TA. Importantly, the

antiradical activity of all the fibers was long-term, persisting up to ~40 days. After immersion in (Concentration of ABTS) ABTS solution, fiber mats looked more damaged than after immersion in DI water. As it was shown in a stability test, the fibers with excess PVP lost their morphology and looked like swollen hydrogel (Figure IV-8 (c)). Only some silhouettes of the fibers can be recognized at the corresponding SEM image. Fibers with stoichiometric amount of PVP and TA (Figure IV-8 (d)) partially retained their morphology, while were thinned, cropped, and wrinkled as a result of their reaction with ABTS solutions. Additionally, the color change of the fibers is noticeable in the insets in Figure IV-8 (c) and (d).

Yellow color acquired the fibers which was deeper at the edges, is similar to the color of oxidized TA. The color and morphology change suggest that TA was partially oxidized in the fibers after reducing the radical species.

The difference in the amount of ABTS radicals per different fibers is not very, which probably means that not all TA is available for the reaction, but only TA in the closer proximity to the solution. The depth of radical penetration is limited by diffusion of the radical into fiber mats

CHAPTER V

MECHANICAL PROPERTIES OF HYDROGEN BONDED COMPLEX NANOFIBERS

Introduction

The evolution of mechanical properties of electrospun nanofibers fall into two categories: testing the macroscopic properties of nanofiber mat and testing the microscopic properties of individual nanofibers on the micron scale.

Macro-Scale Testing

There are multiple reports of simple mechanical testing of various electrospun materials. Usually, the results are reported in terms of engineering stress and engineering

strain, despite the fact that electrospun materials typically experience large deformations. [16, 17] Some groups have performed more rigorous characterization of electrospun materials. Nerurkar et al. developed a constitutive model for aligned PCL scaffolds from uniaxial tests that describes the material as a composite of electrospun fibers and a fluid matrix.[19] Baker et al. developed a similar composite model for combinations of multiple fiber types in a fluid matrix from uniaxial testing data.[6] Others have performed biaxial testing of electrospun scaffolds and have developed elaborate macroscopic constitutive models that factor in the overall fiber alignment, direction of loading, density of fiber interactions, and fiber tortuosity.[13] Duling *et al.* succeeded in characterizing the viscoelastic properties of macroscopic electrospun sheets using the quasi-linear viscoelasticity model.[21, 22] Barocas *et al.* developed a constitutive model for electrospun scaffolds by combining a representative volume element with the Cauchy stress tensor using uniaxial testing data.[23] The primary limitation of the constitutive models developed by these groups is the difficulty in linking the model to the deformations an adherent cell would experience on an electrospun substrate. While these models provide an excellent representation of the average

properties of the material as a whole, the specific strains on a cell cannot be determined from the models alone due to the inherently complex scaffold geometry.

Testing of Individual Electrospun Fibers

Due to the multiple variables that influence the macroscopic mechanical properties of electrospun materials, testing of isolated fibers is the ideal method of determining the intrinsic mechanical properties of the material. Working with individual micro and nanofibers presents a significant handling challenge. Consequently, there are few examples of direct testing of individual electrospun fibers. Individual fiber testing was first reported by Tan et al. in 2004 using an AFM probe to apply micron level displacements.[24] Other methods of single fiber testing include: using AFM probe to bend fibers deposited over a microchannel, individual fibers in a tensile testing apparatus, and using microelectromechanical systems combined with AFM.[25-28] The majority of the reports of individual fiber testing characterize the fiber in terms of engineering stress and engineering strain,[27-29] however, Baker et al. has recently examined both the tensile and viscoelastic properties of dry electrospun fibrinogen fibers and recorded true stress and true strain.[30] The main limitation of single fiber mechanical tests is the inability to test fibers with adherent cells. Thus, any cell-substrate interaction cannot be tested using this method.

Macroscopic testing of electrospun materials has the advantage of better matching the organ-level deformations that are seen in vivo. Nevertheless, microscopic testing seeks to understand the forces cells experience while seeded on the material. Understanding the cellular-level forces present in electrospun constructs is an important, and often overlooked, aspect of the biocompatibility of the material.

Materials and Methods

Chemicals and Instruments Used

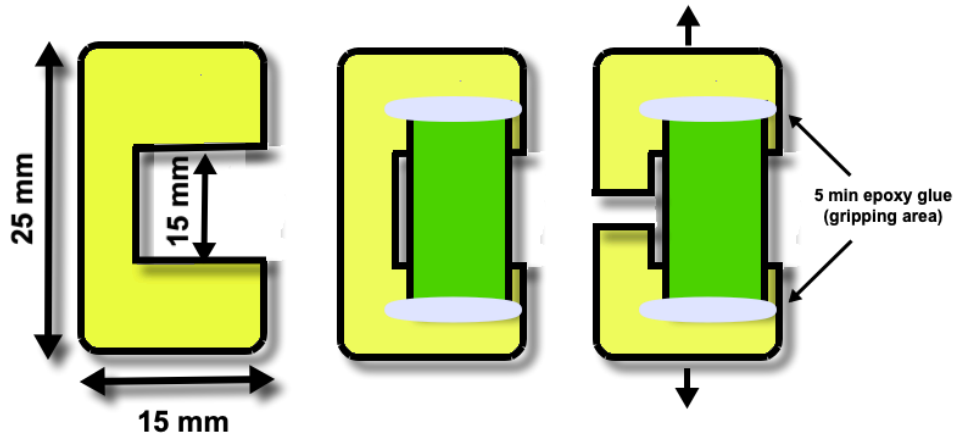

Figure V-1. Schematic representation of a cardboard scaffold made as a supportive mat for mechanical testing. The yellow diagonal pattern demonstrates the scaffold section and the green part resembles the fiber mat.

The nanofiber mat was cut in rectangular shape of dimensions 17 mm x 9 mm (as shown in Figure V-1), and thickness of the fiber film was measured using digital micrometer with the precision of 1 μm. Glass coverslips were used to increase the contact area and reduce the compression of the fiber mat. The micrometer gauge also prevents the application of excess pressure on the mat during measuring by locking itself up after sufficient amount of stress.

The electrospun fibers mats were supported on a C-shaped cardboard frame with dimension of 25 mm x 15 mm. The fiber mat was glued to the scaffold using a special 5 minutes curing time epoxy adhesive carefully. The strength, strain and Young's modulus of specimens were determined through a tensile testing which was carried out using a tensile tester (Gatan MT 10365, Deban UK Ltd). The scaffold with nanofiber on it were carefully attached between the jaws of

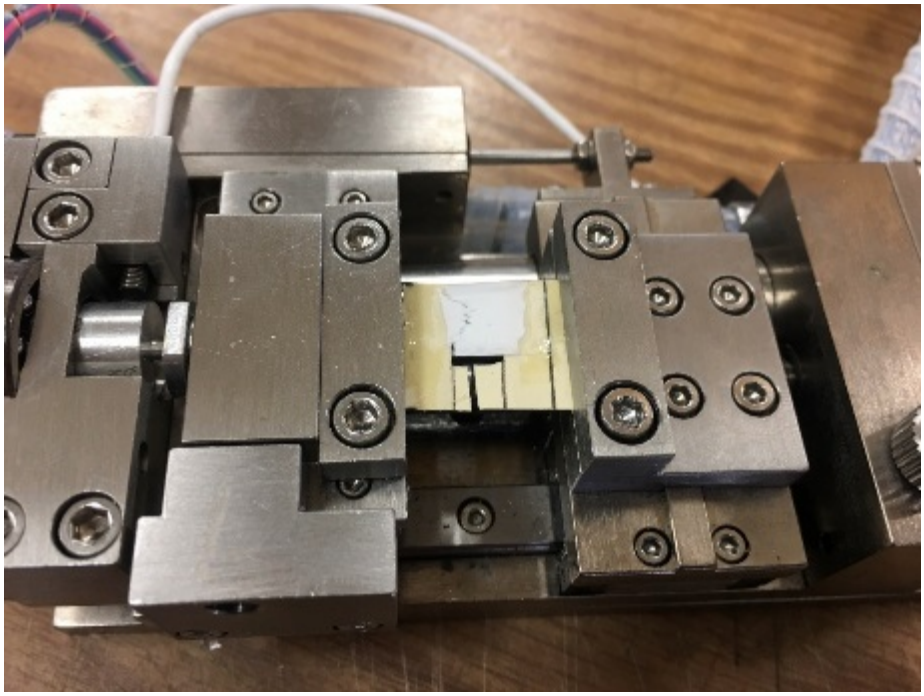

Figure V-2. Gatan tensile tester along with a nanofiber scaffold attached.

tensile tester as shown in Figure V-2. The joint at C-section were carefully cut using a stainless-steel blade without damaging the nanofiber mat. The experiments were realized in the tensile mode at constant speed of 0.5 mm/min and at room temperature and dry conditions. 5 samples were tested and out of which 3 best samples with consistent data were selected for analyzation and data processing.

Results and Discussion

Macroscopic Mechanical Properties

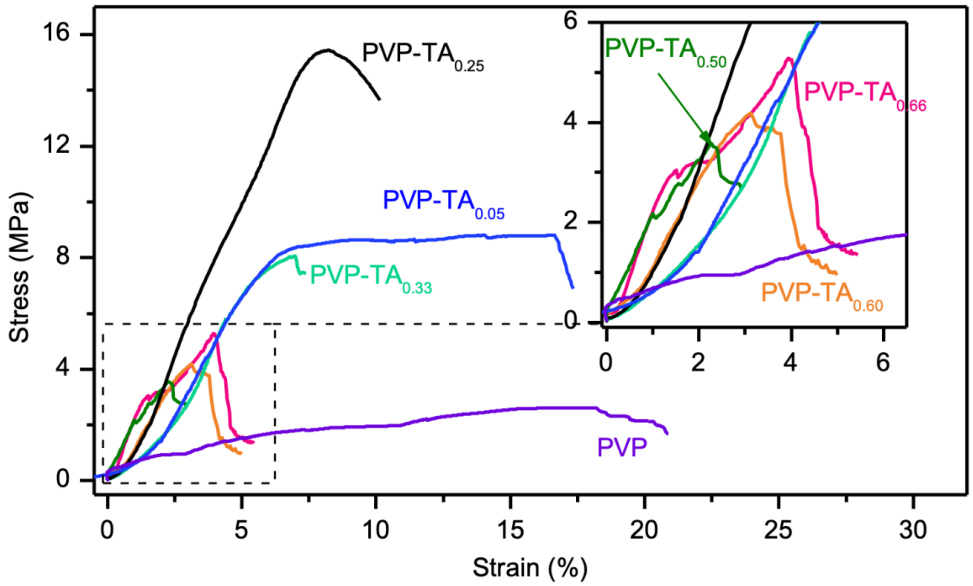

Figure V-3. Representative stress *vs*. strain curve of the tensile test of the fiber mats made of the HBC with the different content of PVP (1300k) and TA.

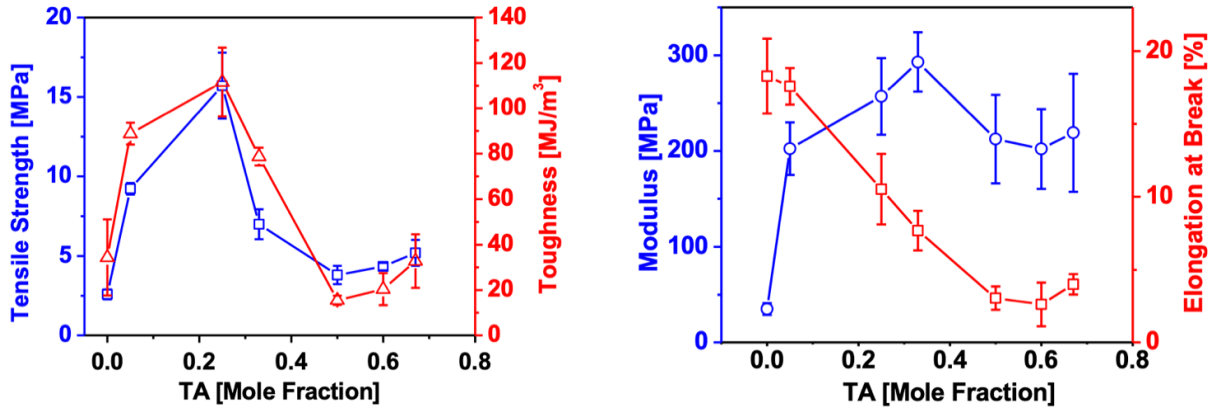

Figure V-4. a) Tensile strength and Toughness and (b) modulus and elongation at break of uniaxially aligned free-standing fiber mats of PVP (1300k) - TA complexes as a function of mole fraction of TA tested at ambient conditions of 24ºC and 50% RH.

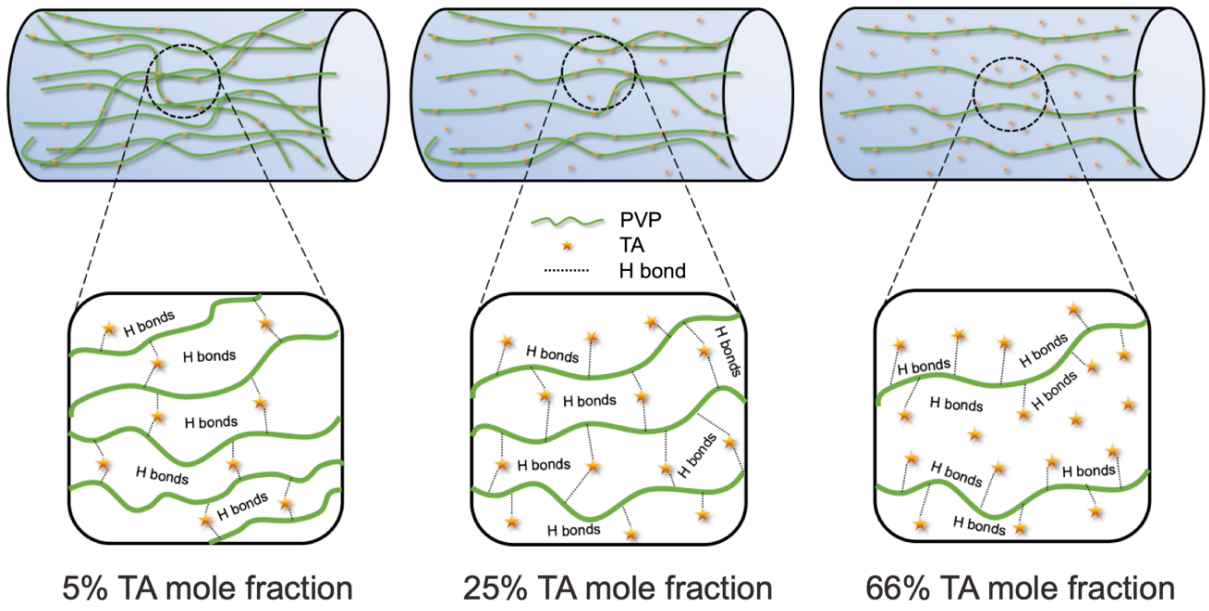

Figure V-5. Schematic representation of effect of fraction of TA in PVP (1300k) – TA at equimolar ratio on mechanical properties of fibers.

To study the effect of PVP-TA hydrogen bonding on macroscopic mechanical properties of the fibers during longitudinal tensile deformation, mats of uniaxially aligned fibers made with various PVP-to-TA ratios were examined. Figure V-4 shows the dependencies of tensile strength, elastic modulus and elongation at break as a function of mole fraction of TA in PVP-TA electrospinning solutions. The stress-strain curves for these measurements are shown in Figure V-3. Mechanical properties of the electrospun nanofibers were measured using the method described in the Experimental Section. To that end, for a chosen constant molecular weight of PVP (Mw = 1300k), tensile strength, toughness, elastic modulus and % elongation at break were determined.

Results in Figure V-3 shows that the tensile strength and Young's modules of pristine PVP (1300k) fibers (2.6 MPa, and13.7 MPa, respectively) sharply increase upon addition of only 0.05 mole fraction of TA. This trend persists till the mole fraction of TA is further increased to ~0.3. However, after a maximum value of 15.7 MPa and 183.9 MPa were achieved at the mole fractions

of 0.25 and 0.33 for tensile strength and Young's modulus, respectively, the materials strength was reduced. Note that the fibers of pristine TA could be prepared because of the low-molecular nature of this molecule. The occurrence of the maxima in the dependences shown in Figure V-3 can be explained by the changes in the density of the hydrogen bonds in the system as shown in Figure V-5 schematically. Specifically, the number of hydrogen bonds between PVP and TA is expected to be maximized at the close-to-equimolar PVP (1300k) - TA molar ratios. Lowering of hydrogen bond density at high molar fraction of TA resulted in deterioration of the fiber strength. In contrast to previously studied PVP-TA interactions in aqueous solution, where equimolar ratio of functional groups resulted in the strongest precipitation of the complexes,[68] in this work the maximum in the tensile strength and Young's modulus occurs at ~3:1 ratio of PVP to TA hydrogen bonding group. The difference in the stoichiometry is likely due to the different hydration state of PVP and TA in these two systems.

The establishment of the network of non-covalent crosslinks upon the addition of TA has improved the tensile strength and Young's modulus of the PVP (1300k) - TA nanofibers, as hydrogen bond interactions between PVP and TA contributed towards an increase in resistance to mechanical deformation and fiber reinforcing. In agreement with previous reports of the effect of hydrogen bonding on mechanical properties of self-assembled polymer materials were reported for other systems,[50, 85, 95] a network of hydrogen bonds also caused a reduction in elongation at break of the fibers from the 18.3% elongation at break for pristine PVP as the fraction of TA was increased. Note that at high molar fraction of TA, elongation at break continued to deteriorate because of the non-polymeric nature of TA molecules.

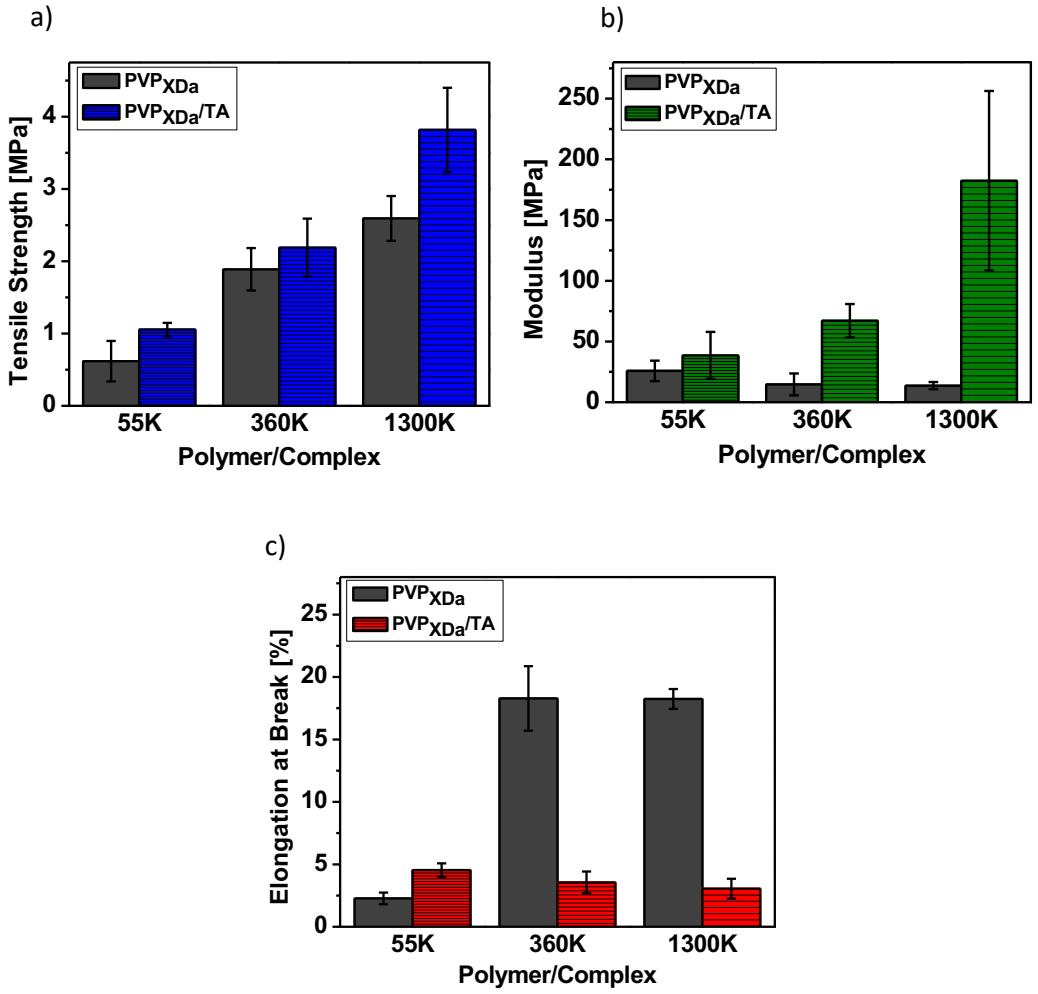

Figure V-6. Variation of mechanical properties as a function of molecular weight of PVP in PVP/TA IPC at equimolar ratio a) tensile strength b) Youngs modulus c) elongation at break.

Same trend was observed in modulus but the maximum point slightly shifted to lower PVP mole fraction (0.66), which might be due to some experimental error. In addition, some fluctuations in mechanical test data for hydrogen-bond systems has been reported by others[50]. The dynamic nature of hydrogen bond systems which make it easier for them to break and reform upon applying mechanical load could be the reason. In case of elongation at break, adding more polymer molecules into the system makes it more flexible and even for highest-strength fibers, the excess

of polymer portion dominates over H-bond interactions and the trend of increasing is still observed. Being a very small molecule, contribution of TA towards elongation is very negligible though.

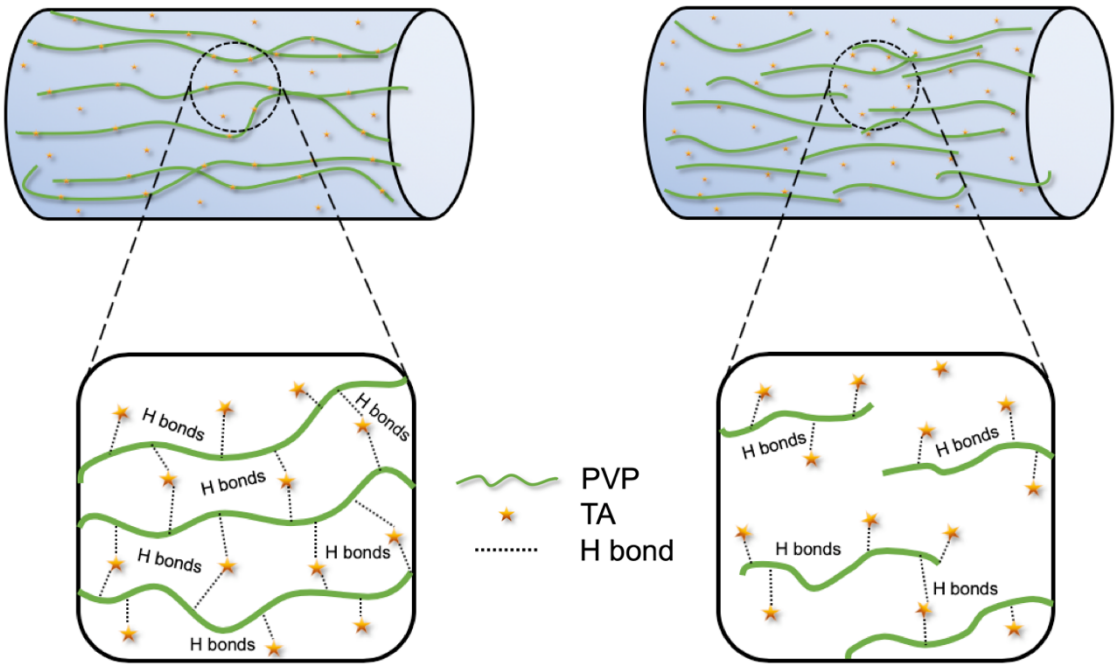

Figure V-7. Schematic representation of the effect variation of molecular weights of PVP on PVP/TA hydrogen bonded IPCs (Left scheme shows the PVP with 1300k and right one shows PVP with (55k)).

Additionally, we studied the mechanical properties of uniaxially aligned complex fibers with varied molecular weight of PVP and compare them with control fibers of PVP, the results are shown in Figure V-6. Results revealed that the average tensile strength of PVP complex nanofibers is more than control nanofibers. PVP chains being more flexible, when introduced with TA, become more rigid. TA acts as a crosslinking point between these chains. In addition, as the molecular weight of long chain molecule increases, the tensile strength and elastic modulus go on increasing. In low molecular weight PVP-TA complex fibers, the short chains of PVP are not

capable and stretched enough to bridge adjacent TA molecules whereas in case of high molecular weight PVP, the long chains are able to maintain the integrity of fibers during elongation (Figure V-7).

Note that the data shown in all the figures present the values for the nominal tensile strength and Young's modulus, which were calculated for the effective cross-section of the fiber mats composed of 70-75% of air (calculated from the fiber density of 0.25-0.30 g/cm^3). However, even in this representation, the tensile strength of the PVP (1300k) - $TA_{0.33}$ fibers is ~three-fold high than the one measured for extruded fibers of hydrogen-bonded PAA/PEO complexes[96] and ~15-fold high that measured with electrospun fibers of hydrogen-bonded complexes of elastin and segmented polyurethane containing polyethylene oxide and poly(L-lactic acid) in their backbone.[50, 96]

CHAPTER VI

CONCLUSION

This study explored a new route of incorporating chemical functionality within polymer nanofibers. Specifically, highly functional polymer nanofibers were synthesized *via* electrospinning of solutions of polyvinylpyrrolidone (PVP) with different molecular weights and a hydrogen-bonding partner, tannic acid (TA). Hydrogen bonding between PVP and TA was revealed from the disappearance of the glass transition temperature of PVP/TA as compared to fibers of pristine PVP. The fiber diameters, stability in aqueous environment and mechanical properties could be all controlled by concentration of PVP, the molar ratio between PVP and TA units, as well as molecular weight of PVP. The role of a network of hydrogen bonds has been revealed in the mechanical behavior of the uniaxially spun fiber mats. Incorporation of a small molecule improved the mechanical properties of pristine PVP radically due to the hydrogen bonding. Mechanical properties of fibers were found to be dependent on the molar ratios between PVP-TA and molecular weight of PVP chains. Unlike in an aqueous solution where maximum hydrogen bonding interactions occur at equimolar ratio, in electrospun PVP-TA fibers, maxima in mechanical properties occurred at 0.25 molar fraction of TA. Also, the incorporation of long chain PVP in PVP-TA complex improved tensile and modulus properties fibers. Moreover, PVP-TA fiber mats exhibited unprecedented prolonged antioxidant activity, showing promise for their application for scavenging free radicals in solution.

REFERENCES

1. Parthasarathi, R.; Subramanian, V.; Sathyamurthy, N., Hydrogen bonding without borders: an atoms-in-molecules perspective. *The Journal of Physical Chemistry A* **2006,** *110* (10), 3349-3351.

2. Meot-Ner, M., The ionic hydrogen bond. *Chem. Rev.* **2005,** *105* (1), 213-284.

3. Kollman, P. A.; Allen, L. C., Theory of the hydrogen bond. *Chem. Rev.* **1972,** *72* (3), 283-303.

4. Ikawa, T.; Abe, K.; Honda, K.; Tsuchida, E., Interpolymer complex between poly (ethylene oxide) and poly (carboxylic acid). *Journal of Polymer Science: Polymer Chemistry Edition* **1975,** *13* (7), 1505-1514.

5. Khutoryanskiy, V. V., Hydrogen-bonded interpolymer complexes as materials for pharmaceutical applications. *Int. J. Pharm.* **2007,** *334* (1-2), 15-26.

6. Jiang, M.; Li, M.; Xiang, M.; Zhou, H., Interpolymer complexation and miscibility enhancement by hydrogen bonding. In *Polymer Synthesis/Polymer-Polymer Complexation*, Springer: 1999; pp 121-196.

7. Abe, K.; Ohno, H.; Nii, A.; Tsuchida, E., Calorimetric study on the formation of polymer complexes through electrostatic interaction and hydrogen bonding. *Die Makromolekulare Chemie: Macromolecular Chemistry and Physics* **1978,** *179* (8), 2043-2050.

8. Dubolazov, A.; Nurkeeva, Z.; Mun, G.; Lukmanova, D.; Khutoryanskiy, V., Temperature effect on solution properties of interpolymer complexes based on poly (acrylic acid) and some cellulose ethers. *Euras. Chem. Technol. J* **2004,** *6* (299-303), 2005.

9. Khutoryanskiy, V. V.; Nurkeeva, Z. S.; Mun, G. A.; Dubolazov, A. V., Effect of temperature on aggregation/dissociation behavior of interpolymer complexes stabilized by hydrogen bonds. *J. Appl. Polym. Sci.* **2004,** *93* (4), 1946-1950.

10. Staikos, G.; Karayanni, K.; Mylonas, Y., Complexation of polyacrylamide and poly (N-isopropylacrylamide) with poly (acrylic acid). The temperature effect. *Macromol. Chem. Phys.* **1997,** *198* (9), 2905-2915.

11. DeLongchamp, D. M.; Hammond, P. T., Highly ion conductive poly (ethylene oxide)-based solid polymer electrolytes from hydrogen bonding layer-by-layer assembly. *Langmuir* **2004,** *20* (13), 5403-5411.

12. Shulga, G.; Rekner, F.; Varslavan, J., SW—soil and water: Lignin-based interpolymer complexes as a novel adhesive for protection against erosion of sandy soil. *Journal of agricultural engineering research* **2001,** *78* (3), 309-316.

13. Orazzhanova, L.; Yashkarova, M.; Bimendina, L.; Kudaibergenov, S., Binary and ternary polymer–strontium complexes and the capture of radioactive strontium-90 from the polluted soil of the Semipalatinsk Nuclear Test Site. *J. Appl. Polym. Sci.* **2003,** *87* (5), 759-764.

14. Chen, J.-P.; Chang, G.-Y.; Chen, J.-K., Electrospun collagen/chitosan nanofibrous membrane as wound dressing. *Colloids Surf. Physicochem. Eng. Aspects* **2008,** *313*, 183-188.

15. Kurokawa, Y.; Ueno, K.; Yui, N., Reverse osmosis rejection of organic solute from aqueous solution by using cellulose acetate phthalate-polyvinylpyrolidone membrane. *J. Colloid Interface Sci.* **1980,** *74* (2), 561-563.

16. Ghasemi-Mobarakeh, L.; Prabhakaran, M. P.; Morshed, M.; Nasr-Esfahani, M.-H.; Ramakrishna, S., Electrospun poly (ε-caprolactone)/gelatin nanofibrous scaffolds for nerve tissue engineering. *Biomaterials* **2008,** *29* (34), 4532-4539.

17. Suja, P.; Reshmi, C.; Sagitha, P.; Sujith, A., Electrospun nanofibrous membranes for water purification. *Polymer Reviews* **2017,** *57* (3), 467-504.

18. Thenmozhi, S.; Dharmaraj, N.; Kadirvelu, K.; Kim, H. Y., Electrospun nanofibers: new generation materials for advanced applications. *Materials Science and Engineering: B* **2017,** *217*, 36-48.

19. Bai, J.; Li, Y.; Yang, S.; Du, J.; Wang, S.; Zheng, J.; Wang, Y.; Yang, Q.; Chen, X.; Jing, X., A simple and effective route for the preparation of poly (vinylalcohol)(PVA) nanofibers containing gold nanoparticles by electrospinning method. *Solid State Commun.* **2007,** *141* (5), 292-295.

20. Lannutti, J.; Reneker, D.; Ma, T.; Tomasko, D.; Farson, D., Electrospinning for tissue engineering scaffolds. *Materials Science and Engineering: C* **2007,** *27* (3), 504-509.

21. Cui, W.; Li, X.; Zhou, S.; Weng, J., Investigation on process parameters of electrospinning system through orthogonal experimental design. *J. Appl. Polym. Sci.* **2007,** *103* (5), 3105-3112.

22. Matthews, J. A.; Wnek, G. E.; Simpson, D. G.; Bowlin, G. L., Electrospinning of collagen nanofibers. *Biomacromolecules* **2002,** *3* (2), 232-238.

23. Shin, Y.; Hohman, M.; Brenner, M.; Rutledge, G., Experimental characterization of electrospinning: the electrically forced jet and instabilities. *Polymer* **2001,** *42* (25), 09955-09967.

24. Li, D.; Xia, Y., Electrospinning of nanofibers: reinventing the wheel? *Advanced materials* **2004,** *16* (14), 1151-1170.

25. Huang, Z.-M.; Zhang, Y.-Z.; Kotaki, M.; Ramakrishna, S., A review on polymer nanofibers by electrospinning and their applications in nanocomposites. *Compos. Sci. Technol.* **2003,** *63* (15), 2223-2253.

26. Tan, S.; Inai, R.; Kotaki, M.; Ramakrishna, S., Systematic parameter study for ultra-fine fiber fabrication via electrospinning process. *Polymer* **2005,** *46* (16), 6128-6134.

27. Zong, X.; Kim, K.; Fang, D.; Ran, S.; Hsiao, B. S.; Chu, B., Structure and process relationship of electrospun bioabsorbable nanofiber membranes. *Polymer* **2002,** *43* (16), 4403-4412.

28. Fong, H.; Chun, I.; Reneker, D., Beaded nanofibers formed during electrospinning. *Polymer* **1999,** *40* (16), 4585-4592.

29. Lee, J. S.; Choi, K. H.; Ghim, H. D.; Kim, S. S.; Chun, D. H.; Kim, H. Y.; Lyoo, W. S., Role of molecular weight of atactic poly (vinyl alcohol)(PVA) in the structure and properties of PVA nanofabric prepared by electrospinning. *J. Appl. Polym. Sci.* **2004,** *93* (4), 1638-1646.

30. Buchko, C. J.; Chen, L. C.; Shen, Y.; Martin, D. C., Processing and microstructural characterization of porous biocompatible protein polymer thin films. *Polymer* **1999,** *40* (26), 7397-7407.

31. Wang, X.; Cao, J.; Hu, Z.; Pan, W.; Liu, Z., Jet shaping nanofibers and the collection of nanofiber mats in electrospinning. *J. Mater. Sci. Technol.* **2006,** *22* (4), 536-540.

32. Zhao, S.; Wu, X.; Wang, L.; Huang, Y., Electrospinning of ethyl–cyanoethyl cellulose/tetrahydrofuran solutions. *J. Appl. Polym. Sci.* **2004,** *91* (1), 242-246.

33. Mazoochi, T.; Hamadanian, M.; Ahmadi, M.; Jabbari, V., Investigation on the morphological characteristics of nanofiberous membrane as electrospun in the different processing parameters. *International Journal of Industrial Chemistry* **2012,** *3* (1), 2.

34. Ding, W.; Wei, S.; Zhu, J.; Chen, X.; Rutman, D.; Guo, Z., Manipulated electrospun PVA nanofibers with inexpensive salts. *Macromolecular Materials and Engineering* **2010,** *295* (10), 958-965.

35. Bosworth, L. A.; Downes, S., Acetone, a sustainable solvent for electrospinning poly (ε-caprolactone) fibres: effect of varying parameters and solution concentrations on fibre diameter. *J. Polym. Environ.* **2012,** *20* (3), 879-886.

36. Zargham, S.; Bazgir, S.; Tavakoli, A.; Rashidi, A. S.; Damerchely, R., The effect of flow rate on morphology and deposition area of electrospun nylon 6 nanofiber. *Journal of Engineered Fibers and Fabrics* **2012,** *7* (4), 155892501200700414.

37. Milleret, V.; Simona, B.; Neuenschwander, P.; Hall, H., Tuning electrospinning parameters for production of 3D-fiber-fleeces with increased porosity for soft tissue engineering applications. *Eur Cell Mater* **2011,** *21* (1473-2262), 286-303.

38. Wang, C.; Chien, H.-S.; Yan, K.-W.; Hung, C.-L.; Hung, K.-L.; Tsai, S.-J.; Jhang, H.-J., Correlation between processing parameters and microstructure of electrospun poly (D, L-lactic acid) nanofibers. *Polymer* **2009,** *50* (25), 6100-6110.

39. Thompson, C.; Chase, G. G.; Yarin, A.; Reneker, D., Effects of parameters on nanofiber diameter determined from electrospinning model. *Polymer* **2007,** *48* (23), 6913-6922.

40. De Schoenmaker, B.; Van der Schueren, L.; Ceylan, Ö.; De Clerck, K., Electrospun polyamide 4.6 nanofibrous nonwovens: parameter study and characterization. *Journal of Nanomaterials* **2012,** *2012*, 14.

41. Lin, Y.; Cai, W.; Tian, X.; Liu, X.; Wang, G.; Liang, C., Polyacrylonitrile/ferrous chloride composite porous nanofibers and their strong Cr-removal performance. *J. Mater. Chem.* **2011,** *21* (4), 991-997.

42. Chen, L.-F.; Zhang, X.-D.; Liang, H.-W.; Kong, M.; Guan, Q.-F.; Chen, P.; Wu, Z.-Y.; Yu, S.-H., Synthesis of nitrogen-doped porous carbon nanofibers as an efficient electrode material for supercapacitors. *ACS nano* **2012,** *6* (8), 7092-7102.

43. Amiraliyan, N.; Nouri, M.; Kish, M. H., Electrospinning of silk nanofibers. I. An investigation of nanofiber morphology and process optimization using response surface methodology. *Fibers and Polymers* **2009,** *10* (2), 167-176.

44. Reneker, D.; Kataphinan, W.; Theron, A.; Zussman, E.; Yarin, A., Nanofiber garlands of polycaprolactone by electrospinning. *Polymer* **2002,** *43* (25), 6785-6794.

45. Iwamoto, S.; Kai, W.; Isogai, A.; Iwata, T., Elastic modulus of single cellulose microfibrils from tunicate measured by atomic force microscopy. *Biomacromolecules* **2009,** *10* (9), 2571-2576.

46. Stachewicz, U.; Barber, A. H., Enhanced wetting behavior at electrospun polyamide nanofiber surfaces. *Langmuir* **2011,** *27* (6), 3024-3029.

47. Ngadiman, N. H. A.; Noordin, M.; Idris, A.; Shakir, A. S. A.; Kurniawan, D., Influence of polyvinyl alcohol molecular weight on the electrospun nanofiber mechanical properties. *Procedia Manufacturing* **2015,** *2*, 568-572.

48. Huang, Z.-M.; Zhang, Y.; Ramakrishna, S.; Lim, C., Electrospinning and mechanical characterization of gelatin nanofibers. *Polymer* **2004,** *45* (15), 5361-5368.

49. Zhang, X.; Nakagawa, R.; Chan, K. H. K.; Kotaki, M., Mechanical property enhancement of polylactide nanofibers through optimization of molecular weight, electrospinning conditions, and stereocomplexation. *Macromolecules* **2012,** *45* (13), 5494-5500.

50. Heiny, M.; Shastri, V. P., Nanofibers of Elastin and Hydrophilic Segmented Polyurethane Solution Blends Show Enhanced Mechanical Properties through Intermolecular Protein–Polymer H Bonding. *Biomacromolecules* **2016,** *17* (4), 1312-1320.

51. Ding, W.; Calabri, L.; Chen, X.; Kohlhaas, K. M.; Ruoff, R. S., Mechanics of crystalline boron nanowires. *Compos. Sci. Technol.* **2006,** *66* (9), 1112-1124.

52. Zussman, E.; Burman, M.; Yarin, A.; Khalfin, R.; Cohen, Y., Tensile deformation of electrospun nylon-6, 6 nanofibers. *J. Polym. Sci., Part B: Polym. Phys.* **2006,** *44* (10), 1482-1489.

53. Lekka, M.; Laidler, P.; Gil, D.; Lekki, J.; Stachura, Z.; Hrynkiewicz, A., Elasticity of normal and cancerous human bladder cells studied by scanning force microscopy. *Eur. Biophys. J.* **1999,** *28* (4), 312-316.

54. Guck, J.; Schinkinger, S.; Lincoln, B.; Wottawah, F.; Ebert, S.; Romeyke, M.; Lenz, D.; Erickson, H. M.; Ananthakrishnan, R.; Mitchell, D., Optical deformability as an inherent cell marker for testing malignant transformation and metastatic competence. *Biophys. J.* **2005,** *88* (5), 3689-3698.

55. Zhang, Y.; Venugopal, J.; Huang, Z.-M.; Lim, C.; Ramakrishna, S., Crosslinking of the electrospun gelatin nanofibers. *Polymer* **2006,** *47* (8), 2911-2917.

56. Schiffman, J. D.; Schauer, C. L., Cross-linking chitosan nanofibers. *Biomacromolecules* **2007,** *8* (2), 594-601.

57. Sukhishvili, S. A.; Granick, S., Layered, erasable, ultrathin polymer films. *J. Am. Chem. Soc.* **2000,** *122* (39), 9550-9551.

58. Sukhishvili, S. A.; Granick, S., Layered, erasable polymer multilayers formed by hydrogen-bonded sequential self-assembly. *Macromolecules* **2002,** *35* (1), 301-310.

59. Such, G. K.; Johnston, A. P.; Caruso, F., Engineered hydrogen-bonded polymer multilayers: from assembly to biomedical applications. *Chem. Soc. Rev.* **2010,** *40* (1), 19-29.

60. Kharlampieva, E.; Sukhishvili, S. A., Hydrogen-bonded layer-by-layer polymer films. *Journal of Macromolecular Science, Part C: Polymer Reviews* **2006,** *46* (4), 377-395.

61. Kim, B.-S.; Lee, H.-i.; Min, Y.; Poon, Z.; Hammond, P. T., Hydrogen-bonded multilayer of pH-responsive polymeric micelles with tannic acid for surface drug delivery. *Chem. Commun.* **2009,** (28), 4194-4196.

62. Zhu, Z.; Gao, N.; Wang, H.; Sukhishvili, S. A., Temperature-triggered on-demand drug release enabled by hydrogen-bonded multilayers of block copolymer micelles. *J. Controlled Release* **2013,** *171* (1), 73-80.

63. Xiang, F.; Ward, S. M.; Givens, T. M.; Grunlan, J. C., Structural tailoring of hydrogen-bonded poly (acrylic acid)/poly (ethylene oxide) multilayer thin films for reduced gas permeability. *Soft matter* **2015,** *11* (5), 1001-1007.

64. Yang, S. Y.; Rubner, M. F., Micropatterning of polymer thin films with pH-sensitive and cross-linkable hydrogen-bonded polyelectrolyte multilayers. *J. Am. Chem. Soc.* **2002,** *124* (10), 2100-2101.

65. Feldstein, M. M.; Bovaldinova, K. A.; Bermesheva, E. V.; Moscalets, A. P.; Dormidontova, E. E.; Grinberg, V. Y.; Khokhlov, A. R., Thermo-switchable pressure-sensitive adhesives based on poly (N-vinyl caprolactam) non-covalently cross-linked by poly (ethylene glycol). *Macromolecules* **2014,** *47* (16), 5759-5767.

66. Smith, K.; Winslow, A.; Petersen, D., Association reactions for poly (alkylene oxides) and polymeric poly (carboxylic acids). *Industrial & Engineering Chemistry* **1959,** *51* (11), 1361-1364.

67. Kim, B.-S.; Park, S. W.; Hammond, P. T., Hydrogen-bonding layer-by-layer-assembled biodegradable polymeric micelles as drug delivery vehicles from surfaces. *ACS nano* **2008,** *2* (2), 386-392.

68. Erel-Unal, I.; Sukhishvili, S. A., Hydrogen-Bonded Multilayers of a Neutral Polymer and a Polyphenol. *Macromolecules* **2008,** *41* (11), 3962-3970.

69. Chen, K.-S.; Hsiao, Y.-C.; Kuo, D.-Y.; Chou, M.-C.; Chu, S.-C.; Hsieh, Y.-S.; Lin, T.-H., Tannic acid-induced apoptosis and-enhanced sensitivity to arsenic trioxide in human leukemia HL-60 cells. *Leukemia Res.* **2009,** *33* (2), 297-307.

70. Sakagami, H.; Jiang, Y.; Kusama, K.; Atsumi, T.; Ueha, T.; Toguchi, M.; Iwakura, I.; Satoh, K.; Ito, H.; Hatano, T., Cytotoxic activity of hydrolyzable tannins against human oral tumor cell lines—a possible mechanism. *Phytomedicine* **2000,** *7* (1), 39-47.

71. Tikoo, K.; Sane, M. S.; Gupta, C., Tannic acid ameliorates doxorubicin-induced cardiotoxicity and potentiates its anti-cancer activity: potential role of tannins in cancer chemotherapy. *Toxicol. Appl. Pharmacol.* **2011,** *251* (3), 191-200.

72. Meng, X.; Perry, S. L.; Schiffman, J. D., Complex Coacervation: Chemically Stable Fibers Electrospun from Aqueous Polyelectrolyte Solutions. *ACS Macro Letters* **2017,** *6* (5), 505-511.

73. Boas, M.; Gradys, A.; Vasilyev, G.; Burman, M.; Zussman, E., Electrospinning polyelectrolyte complexes: pH-responsive fibers. *Soft Matter* **2015,** *11* (9), 1739-1747.

74. Doshi, J.; Reneker, D. H., Electrospinning process and applications of electrospun fibers. *J. Electrostatics* **1995,** *35* (2-3), 151-160.

75. Power, A.; Chandra, S.; Chapman, J., Graphene, electrospun membranes and granular activated carbon for eliminating heavy metals, pesticides and bacteria in water and wastewater treatment processes. *Analyst* **2018,** *143* (23), 5629-5645.

76. Ma, H.; Burger, C.; Hsiao, B. S.; Chu, B., Ultra-fine cellulose nanofibers: new nano-scale materials for water purification. *J. Mater. Chem.* **2011,** *21* (21), 7507-7510.

77. Ma, Z.; Kotaki, M.; Ramakrishna, S., Electrospun cellulose nanofiber as affinity membrane. *J. Membr. Sci.* **2005,** *265* (1-2), 115-123.

78. Pham, Q. P.; Sharma, U.; Mikos, A. G., Electrospinning of polymeric nanofibers for tissue engineering applications: a review. *Tissue Eng.* **2006,** *12* (5), 1197-1211.

79. Xu, C.; Inai, R.; Kotaki, M.; Ramakrishna, S., Electrospun nanofiber fabrication as synthetic extracellular matrix and its potential for vascular tissue engineering. *Tissue Eng.* **2004,** *10* (7-8), 1160-1168.

80. Ma, Z.; Kotaki, M.; Inai, R.; Ramakrishna, S., Potential of nanofiber matrix as tissue-engineering scaffolds. *Tissue Eng.* **2005,** *11* (1-2), 101-109.

81. Sill, T. J.; von Recum, H. A., Electrospinning: applications in drug delivery and tissue engineering. *Biomaterials* **2008,** *29* (13), 1989-2006.

82. Li, C.; Vepari, C.; Jin, H.-J.; Kim, H. J.; Kaplan, D. L., Electrospun silk-BMP-2 scaffolds for bone tissue engineering. *Biomaterials* **2006,** *27* (16), 3115-3124.

83. Miguel, S. P.; Figueira, D. R.; Simões, D.; Ribeiro, M. P.; Coutinho, P.; Ferreira, P.; Correia, I. J., Electrospun polymeric nanofibres as wound dressings: a review. *Colloids Surf. B. Biointerfaces* **2018,** *169*, 60-71.

84. Rho, K. S.; Jeong, L.; Lee, G.; Seo, B.-M.; Park, Y. J.; Hong, S.-D.; Roh, S.; Cho, J. J.; Park, W. H.; Min, B.-M., Electrospinning of collagen nanofibers: effects on the behavior of normal human keratinocytes and early-stage wound healing. *Biomaterials* **2006,** *27* (8), 1452-1461.

85. Cai, Z.-x.; Mo, X.-m.; Zhang, K.-h.; Fan, L.-p.; Yin, A.-l.; He, C.-l.; Wang, H.-s., Fabrication of chitosan/silk fibroin composite nanofibers for wound-dressing applications. *International journal of molecular sciences* **2010,** *11* (9), 3529-3539.

86. Rujitanaroj, P.-o.; Pimpha, N.; Supaphol, P., Wound-dressing materials with antibacterial activity from electrospun gelatin fiber mats containing silver nanoparticles. *Polymer* **2008,** *49* (21), 4723-4732.

87. Huang, D.; Ou, B.; Prior, R. L., The Chemistry behind Antioxidant Capacity Assays. *Journal of Agricultural and Food Chemistry* **2005,** *53* (6), 1841-1856.

88. Ma, S.; Yuan, Q.; Zhang, X.; Yang, S.; Xu, J., Solvent effect on hydrogen-bonded thin film of poly(vinylpyrrolidone) and poly(acrylic acid) prepared by layer-by-layer assembly. *Colloids and Surfaces A: Physicochemical and Engineering Aspects* **2015,** *471*, 11-18.

89. Wang, Y.; He, J.; Aktas, S.; Sukhishvili, S. A.; Kalyon, D. M., Rheological behavior and self-healing of hydrogen-bonded complexes of a triblock Pluronic® copolymer with a weak polyacid. *J. Rheol.* **2017,** *61* (6), 1103-1119.

90. McKee, M. G.; Wilkes, G. L.; Colby, R. H.; Long, T. E., Correlations of solution rheology with electrospun fiber formation of linear and branched polyesters. *Macromolecules* **2004,** *37* (5), 1760-1767.

91. Deitzel, J. M.; Kleinmeyer, J.; Harris, D.; Tan, N. B., The effect of processing variables on the morphology of electrospun nanofibers and textiles. *Polymer* **2001,** *42* (1), 261-272.

92. Xia, Z.; Singh, A.; Kiratitanavit, W.; Mosurkal, R.; Kumar, J.; Nagarajan, R., Unraveling the mechanism of thermal and thermo-oxidative degradation of tannic acid. *Thermochim. Acta* **2015,** *605*, 77-85.

93. Karahan, H. E.; Eyüboğlu, L.; Kıyılar, D.; Demirel, A. L., pH-stability and pH-annealing of H-bonded multilayer films prepared by layer-by-layer spin-assembly. *European Polymer Journal* **2014,** *56*, 159-167.

94. Gülçin, İ.; Huyut, Z.; Elmastaş, M.; Aboul-Enein, H. Y., Radical scavenging and antioxidant activity of tannic acid. *Arabian Journal of Chemistry* **2010,** *3* (1), 43-53.

95. Song, P. a.; Xu, Z.; Guo, Q., Bioinspired strategy to reinforce PVA with improved toughness and thermal properties via hydrogen-bond self-assembly. *ACS Macro Letters* **2013,** *2* (12), 1100-1104.

96. Li, J.; Wang, Z.; Wen, L.; Nie, J.; Yang, S.; Xu, J.; Cheng, S. Z. D., Highly Elastic Fibers Made from Hydrogen-Bonded Polymer Complex. *ACS Macro Letters* **2016,** *5* (7), 814-818.